ARTICLE

DOI: 10.1590/2317-4889201920180129

BJGEO Brazilian Journal of Geology

The Barreiro suite in the central Ribeira Belt (SE-Brazil): a late Tonian tholeiitic intraplate magmatic event in the distal passive margin of the São Francisco Paleocontinent

Monica Heilbron[1,2]*, Caroline Oliveira[1], Marcela Lobato[1], Claudio de Morisson Valeriano[1,2], Ivo Dussin[1], Elton Dantas[3], Antonio Simonetti[4], Henrique Bruno[1], Felipe Corrales[1], Eduardo Socoloff[1]

Abstract

New geochemical, U-Pb, Lu-Hf and Sr-Nd data from the Barreiro Suite metabasites in comparison with enclaves within the distal Andrelândia Group and the orthogranulites of the Juiz de Fora Complex are presented. Geochemical data suggest intraplate setting, with high and low-TiO_2, TDM_{Nd} ages between 1.80 and 1.41 Ga, negative ENd_t and $(^{87}Sr/^{86}Sr)i$ between 0.714 and 0.747. Results contrast with part of the Juiz de Fora Complex enclaves, with island arc tholeiites- calcalkaline basalts (IAT-CAB) geochemical signatures, TDM_{Nd} ages between 2.58 and 2.16 Ga, positive ENd_t values and $(87Sr/86Sr)_i$ between 0.700 and 0.712. U-Pb data for the Barreiro Suite yielded a crystallization age of 766 ± 13 Ma and a metamorphic overprint of 619 ± 6 Ma. The results indicate three episodes of mafic magmatism in the Occidental terrane of the Ribeira Belt. The two older episodes are related to Rhyacian arc evolution (ca. 2.2 to 2.1 Ga) and to the Statherian (ca. 1.7 Ga) tectonics, and occur only within the Juiz de Fora Complex, while the younger ca. 766 Ma episode constrains the timing of distal passive margin evolution. An important implication is that these late Tonian metabasic rocks could have been a source of detrital zircons for the sedimentation along the distal Andrelândia basin.

KEYWORDS: Andrelândia Group; U-Pb; Sm-Nd; Lu-Hf; within-plate basalts.

INTRODUCTION

Tholeiitic mafic rocks are very common in many different tectonic environments, ranging from continental and oceanic plateaus, continental rifts to passive margins and convergent tectonic settings such as magmatic arcs (Pearce & Cann 1973, Pearce *et al.* 1975, Pearce 1983, 1987, Wilson 1989). In high-grade metamorphic terrains, the original tectonic setting is commonly unclear because recrystallization and deformation obscure primary characteristics. In such terrains, the geochemical and isotopic signatures, and the age of mafic rocks are important tools for the determination of their tectonic setting. Geochronological dating also provides additional constraints on the age of genetically-related high-grade metasedimentary units in orogenic belts.

The Ribeira Belt, southeast Brazil, comprises a Neoproterozoic and Early Paleozoic network of orogenic belts that resulted from the amalgamation of Western Gondwana (Fig. 1A), evolving through episodes of diachronous tectonic accretions and continental collisions in Neoproterozoic and Cambrian times. Together with the Araçuaí Belt (Heilbron *et al.* 2004, 2008, 2017a, Pedrosa-Soares *et al.* 2008, Alkmim *et al.* 2017), the Ribeira Belt makes up a 300 km wide and 600 km long deeply eroded orogenic system that runs roughly parallel to the southeastern coast of Brazil (Fig. 1B).

The external zone of this orogenic system comprises the reworked Neoproterozoic passive margin of the São Francisco paleocontinent. Because of intense deformation and metamorphism related to the Brasiliano collage, the metasedimentary units together with syn-depositional magmatic rocks crop out as high-grade gneisses, tectonically interleaved with highly-deformed basement slivers during the collisional episodes.

The Macaúbas and Andrelândia groups (Paciullo *et al.* 2000, Pedrosa Soares *et al.* 1998, 2000) represent the main Neoproterozoic passive margin sedimentary sequences of the Araçuaí and Ribeira belts. They are mainly siliciclastic, and depositional age constraints are mostly based on U-Pb ages of detrital zircons from quartzitic rocks (Valeriano *et al.* 2004, Valladares *et al.* 2004, 2008, Belém *et al.* 2011, Westin & Campos Neto 2013, Degler *et al.* 2017, Frugis & Campos Neto 2018). Results obtained suggest São Francisco craton source rocks, and the main constraint for the maximum possible sedimentation age of these units is the youngest detrital zircon, ranging in age from Tonian to Cryogenian ages. In several studies, the Cryogenian zircons are interpreted reflecting a shift from passive margin to active tectonic setting, with provenance from approaching magmatic

[1]Universidade do Estado do Rio de Janeiro – Rio de Janeiro (RJ), Brazil. E-mails: monica.heilbron@gmail.com, caroline.oliveira.geo@gmail.com, marcelalobato@gmail.com, valeriano.claudio@gmail.com, ivodusin@yahoo.com.br, henrique.bruno1602@gmail.com, eduardo.socoloff@gmail.com

[2]University of Salzburg – Salzburg, Austria.

[3]Universidade de Brasilia – Brasília (DF), Brazil. E-mail: elton@unb.br

[4]University of Notre Dame – South Bend (IN), USA. E-mail: antonio.simonetti.3@nd.edu

*Corresponding author.

arcs (Campos Neto *et al.* 2011, Belém *et al.* 2011, Degler *et al.* 2017). The major problem is that most of these studied units are metamorphosed to upper amphibolite to granulite facies, so many of these young zircons shows complex textures, with internal cores with different ages and compositions, suggestive of metamorphic reworking at high temperature that could lead to Pb loss. Therefore, another tool for constraining the depositional age of these high-grade siliciclastic rocks is the age of syn- or post-depositional magmatic rocks.

This study aims to contribute to the understanding of the development of the distal passive margin of the São Francisco paleocontinent by presenting new geological, geochemical and geochronological data for the Barreiro Suite (Heilbron *et al.* 2012, 2017b). This recently described unit includes tholeiitic mafic rocks that occur within the distal segment of the Andrelândia basin. However, a further toll for constraining the depositional age of these high-grade siliciclastic rocks is the age of syn or post-depositional magmatic rocks. We also present a comparison of geochemical and Sm-Nd and Sr isotope data from metabasic rocks intercalated in the Andrelândia and Macaúbas sequences with data for basic enclaves and layers that occur within the basement units such as the Juiz de Fora Complex.

TECTONIC SETTING: THE ANDRELÂNDIA GROUP IN THE DISTAL SÃO FRANCISCO PASSIVE MARGIN

The study area is located in the central segment of the Neoproterozoic-Cambrian Ribeira Belt (Almeida *et al.* 1981, Heilbron *et al.* 2004). Following the tectonic subdivision of Heilbron *et al.* (2008, 2017a), the Ribeira Belt is divided into four tectono-stratigraphic terranes that sequentially docked against the southeastern portion of the São Francisco paleocontinental passive margin (Fig. 2). From west to east, these terranes are the Occidental Terrane (reworked SFC margin); the Paraíba do Sul-Embú Terrane, docked at ca. 620–595 Ma; the Oriental Terrane, docked at ca. 605–565 Ma; and the Cabo Frio Terrane, docked at ca. 535–510 Ma.

The Occidental Terrane, the focus of this work, is regarded as the reworked passive margin of the São Francisco paleocontinent and comprises three major litho-tectonic units:

- reworked Paleoproterozoic basement and bimodal Mesoproterozoic magmatic rocks (Heilbron *et al.* 1998, 2010, Noce *et al.* 2007, Degler *et al.* 2018);
- a Neoproterozoic metasedimentary sequence described originally as the Andrelândia Group (Paciullo *et al.* 2000);
- syn- to late-collisional Neoproterozoic granitoid rocks (Fig. 2).

Studies carried out in the proximal zone of the Neoproterozoic passive margin (Paciullo 1997, Paciullo *et al.* 2000, Ribeiro *et al.* 1995) proposed a subdivision of the Andrelândia Group into two major sequences. The basal Carrancas Sequence (informal designation) comprises psammitic banded gneisses with quartzites, pelitic schist and amphibolite intercalations (A1 + A2), followed by a regressive succession of quartzites bearing characteristic green muscovite (A3), succeeded by a transgressive succession of graphite-rich grey

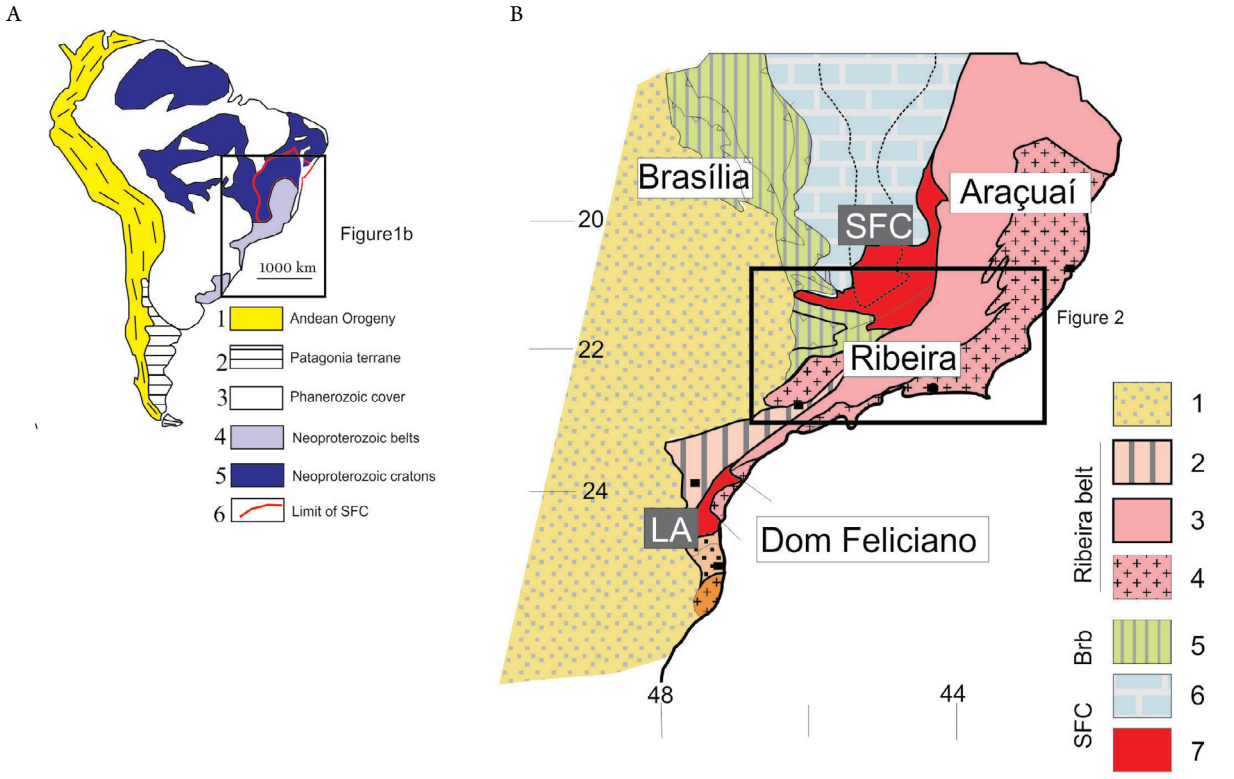

Figure 1. (A) Ribeira Belt in the scenario of South America: 1: Andean Belt; 2: Patagonia terrane; 3: Phanerozoic cover; 4: Cratons; 5: Neoproterozoic belts; 6: São Francisco craton; (B) tectonic organization of SE Brazil: 1: Phanerozoic cover; 2-4: Ribeira Belt units; 2: Apiaí terrane; 3: reworked passive margins; 4: arc-related terranes; 5: Brasília Belt.

schists and feldspathic quartzites (A4). The overlying Serra do Turvo Sequence consists of pelitic schists and gneisses (A6), followed by the uppermost unit of plagioclase-rich schists and gneisses (A5). In the distal segment of the passive margin, where our study is located, only the basal unit (A1 + A2 equivalent?) and a pelitic unit of paragnais and schist (A6) are present. In the recent geological map of Rio de Janeiro State (Heilbron *et al.* 2017b), the name of Raposos Group was adopted for this distal portion of the Andrelândia Group. Because of intense tectonic shuffling with basement rocks of the Juiz de Fora Complex, and metamorphic conditions up granulite facies, the reconstruction of the architecture of this distal basin is difficult.

Major attempts to determine the depositional age of the Andrelândia Group were based on detrital zircons in metasedimentary rocks and on few Sm-Nd model ages of intercalated metabasic rocks (Heilbron *et al.* 1989, Frugis & Campos Neto 2018). Most data point a Tonian onset of sedimentation after ca. 1.0–0.9 Ga (Valeriano *et al.* 2004, Valladares *et al.* 2004. On the other hand, younger Neoproterozoic zircons with ages of ca. 680 Ma for the A5 unit have been attributed to provenance from magmatic arcs during the orogenic stage (Belém *et al.* 2011, Frugis & Campos Neto 2018, Westin & Campos Neto 2013), indicating a shift to an active setting. It is important to stress that high-pressure granulite facies metamorphism between 640 and 600 Ma hampers precise determination of the minimum age of sedimentation (Coelho *et al.* 2017, Heilbron *et al.* 2017a, Trouw *et al.* 2013).

Metabasic rocks are interlayered with the A1 + A2 and A6 units and normally parallel to the primary sedimentary bedding. They vary from fine-grained and foliated amphibolites to coarse-grained mafic granulites. In the high-pressure metamorphic facies, garnet + clinopyroxene + quartz is a very common assemblage in the lower Andrelândia nappe system. Relics of retro-eclogite have been described by Silva *et al.* (2002), Trouw *et al.* (2000, 2013), Campos Neto (2000), and by Coelho *et al.* (2017). In the upper nappe system, referred to Heilbron *et al.* (2000) as the Juiz de Fora crustal duplex system, (garnet) + orthopyroxene + clinopyroxene + quartz is the most common assemblage (Duarte *et al.* 2003).

Gonçalves & Figueiredo (1992) studied mafic rocks that occur near the town of Andrelândia, while Marins (2000) presented geochemical data for mafic rocks located between Conservatória and Barra do Piraí. Both studies report intraplate to MORB-like signatures. A few Sm-Nd model ages of ca. 1.0 Ga were also reported for mafic rocks near Andrelândia town (Heilbron *et al.* 1989).

MAFIC ROCKS OF THE STUDY AREA: GEOLOGY AND PETROGRAPHY

Centimetric to decametric enclaves of metabasic rocks are interlayered within rocks of the Neoproterozoic Andrelândia Group and the orthogranulites of the Juiz de Fora Complex.

The Barreiro Suite is dominated by metabasic bodies shown in the 1:100.000 geological maps of Santo Antônio de Pádua

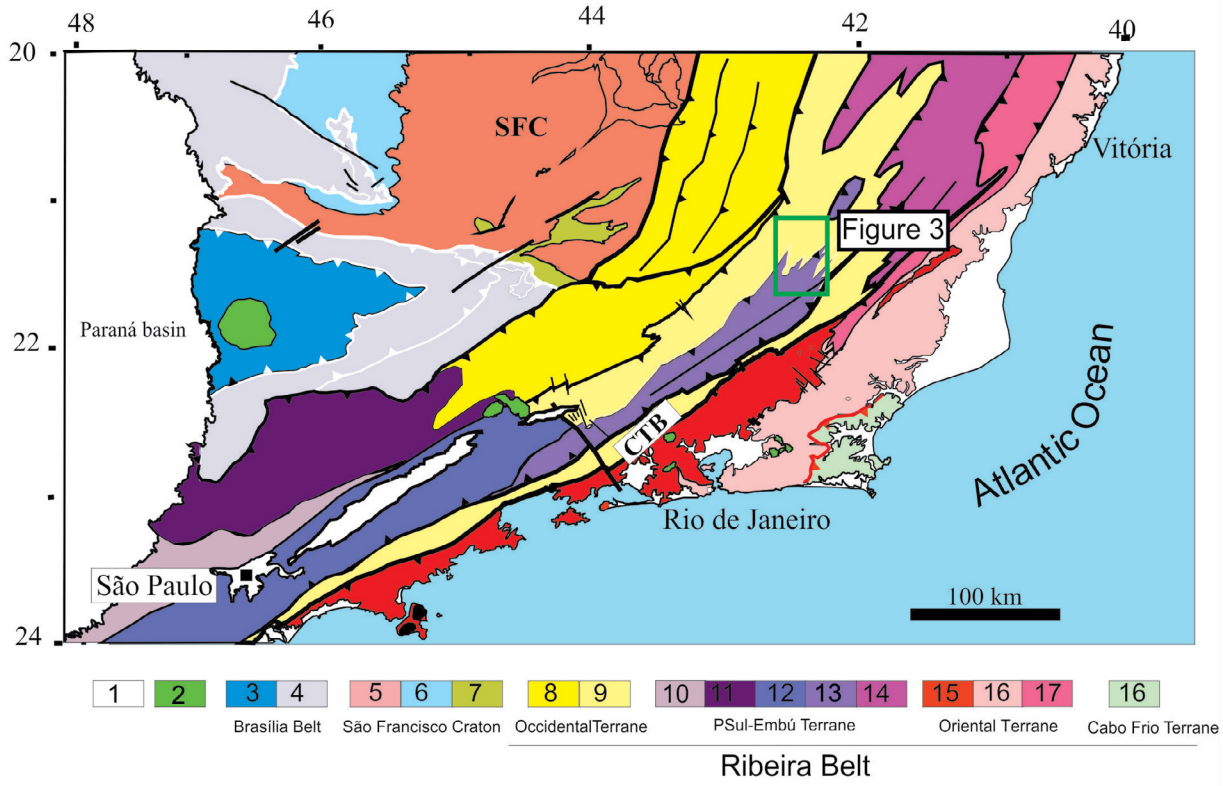

1: Phanerozoic cover; 2: K-T alkaline rocks; 3: passive margin related nappes; 4: arc-related nappes; 5: cratonic basement; 6: Bambuí cover; 7: Mesoproterozoic rift-to-sag units; 8-9: Occidental Terrane with 8 — Andrelândia (lower thrust) and 9 — Juiz de Fora (upper thrust). Cordilleran arc accreted terrane, with 10: Apiaí; 11: Socorro; 12: Embú; 13: Paraíba do Sul; 14: Rio Doce; 15: Rio Negro arc; 16: Italva arc; 17: high-grade metasediments; 18: Cabo Frio Terrane.

Figure 2. Tectonic map of central Ribeira Belt, modified from Heilbron *et al.* (2017a). The green rectangle shows the studied area.

(Heilbron *et al.* 2012) and Ubá (Noce *et al.* 2003) sheets. A decametric-scale mafic body was described within the orthogranulites of the Juiz de Fora Complex. Initially, our work was conducted to date this mafic occurrence. However, our detailed geological mapping shows that the Barreiro suite also occur within the Andrelândia metasedimentary rocks and within the ca. 620–595 Ma syn-collisional garnet charnockites (diatexites) of the Salvaterra suite (Duarte *et al.* 2013) (Fig. 3). The major mafic bodies occur in the western part of the mapped area, as enclaves within this syn-collision Brasiliano granitoid suite. For comparison, these minor lenses within the other country rocks were sampled.

The contact relationships with country rocks are different in the two situations. The lenses in the garnet charnockite, especially the centimentric ones, show textural evidence of partial digestion, suggesting that they are refractory material that survived partial melting.

Mafic lenses within the Andrelândia Group and the Juiz de Fora Complex

The mafic lenses (Figs. 3 and 4) have centimetre to decametre dimensions and display at least two types of relationships with country rocks. Some of the largest bodies display very sharp contacts either with the metasedimentary rocks of the Andrelândia Group, or with the orthogranulites of the Juiz de Fora Complex. On the other hand, centimetric scale enclaves within the orthogranulites show diffuse contacts possibly indicating that they have a common magmatic origin (Fig. 5).

Mafic enclaves are granulite facies rocks, containing ortho and clinopyroxene, and locally garnet (Fig. 5). Hornblende, biotite and plagioclase also occurs, besides accessory phases such as ilmenite, zircon and apatite. Textures vary from granoblastic to mylonitic, compatible with those of the country rocks.

The Barreiro Suite

In the larger (up to 50 m) lenses of the Barreiro Suite (Fig. 4), two lithofacies were observed, consisting respectively of medium to fine- and coarse-grained rocks (Fig. 6). Because of the quality of the outcrops, mainly as quasi in-situ

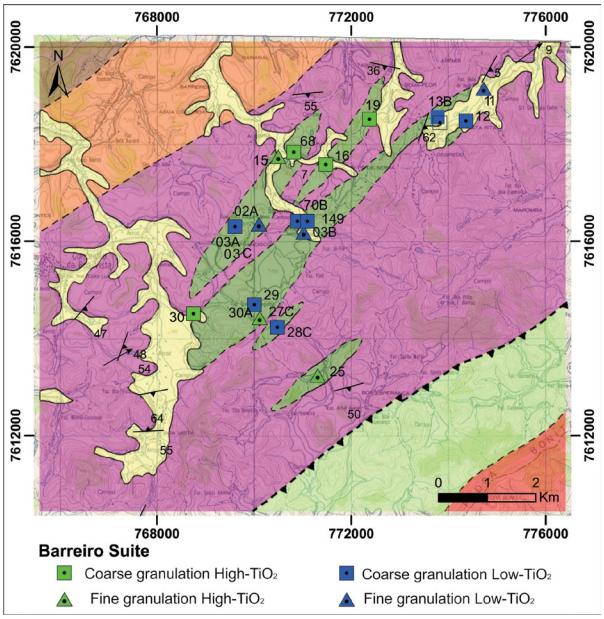

Figure 4. Geological map of the Barreiro Suite, with the location of the analysed rocks. All samples gave the same prefix code RE-CE.

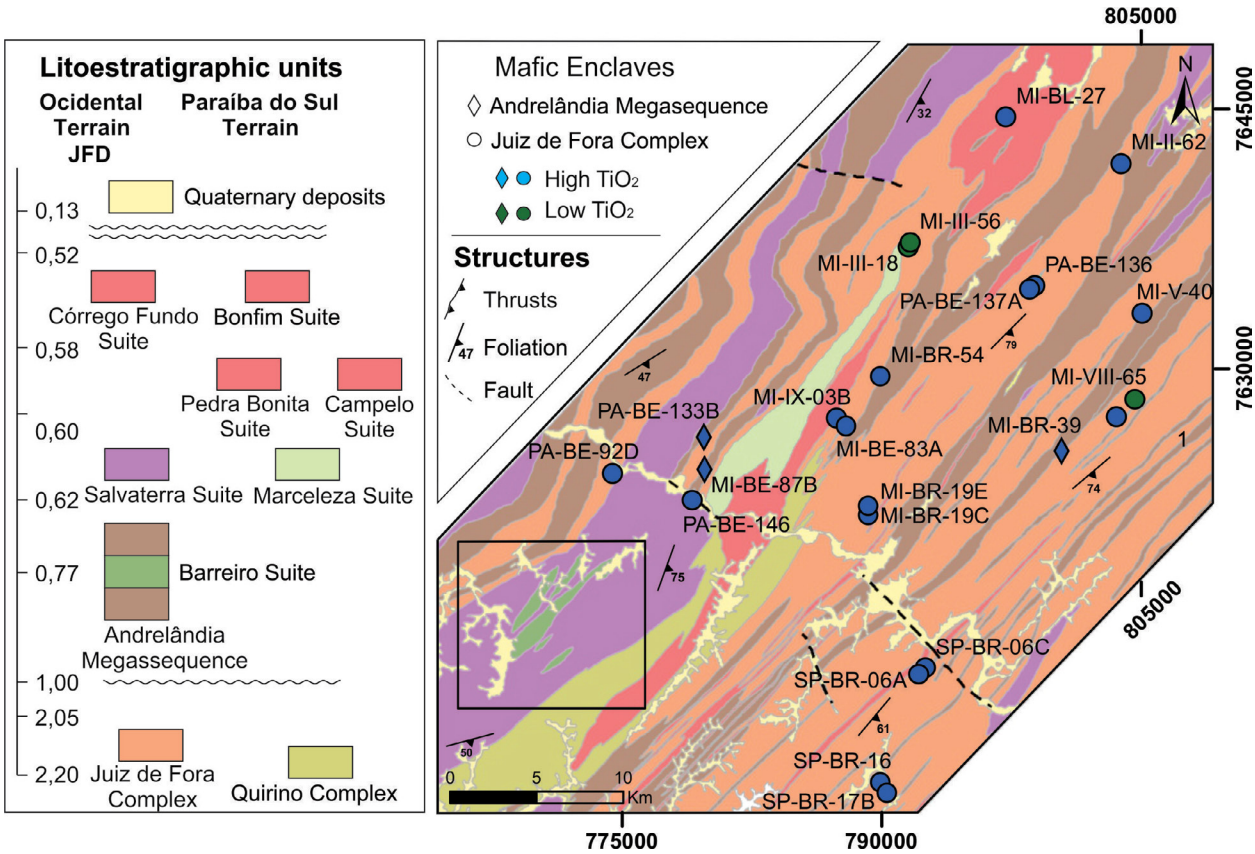

Figure 3. Geological map of the studied area with the location of the analysed enclaves from the country rocks.

mega-boulders, it was not possible to clearly observe the relationships between these two facies. In the field, both occurs as dark gray rocks with a subtle foliation. However, under the microscope, there is a granonematoblastic texture where a visible foliation is defined by the preferential orientation of the mafic minerals. Deformational textures such as incomplete twinning of feldspars, undulose extinction and polygonal granoblastic contacts are commonly observed. The coarse-grained facies rocks locally contain plagioclase porphyroblasts, possibly representing relics of magmatic megacrysts.

The main mineralogy of both facies is represented by orthopyroxene, clinopyroxene, dark hornblende, plagioclase and opaque phases, mainly ilmenite. Biotite and hornblende also occur along the margins of the pyroxenes, suggesting formation by retrogressive reactions. Apatite, quartz and zircon are the common accessory phases.

Geochemistry

Sampling and analytical procedures

Nineteen samples of the metabasic rocks of the Barreiro suite and 23 samples of mafic lenses within Andrelândia Group and Juiz de Fora Complex rocks were selected for geochemical analyses (Tab. 1). Samples were crushed and milled at the Laboratório de Preparação de Amostras (LGPA) of the Universidade do Estado do Rio de Janeiro (UERJ). Activation Laboratories (Ontario, Canada) performed major and trace element analysis, including Rare Earth Elements (REE). Details of the analytical techniques used by this laboratory are presented at www.actlabs.com. Treatment of the data was carried out using the GeoChemical Data ToolKIT (GCDkit) software of Janoušek *et al.* (2006).

RESULTS

The rocks of the Barreiro suite (Tab. 1) range from gabbros to diorites, with silica contents between 47.98 and 54.48%, MgO 2.97–7.45%, and TiO_2 1.72-3.77. They define a subalkaline tholeiitic series that can be subdivided into high (> 2.2%) and low-TiO_2 (< 2.2%) groups (Fig. 7). Both geochemical groups are recognized in both the coarse-and fine-grained varieties of the Barreiro suite. As expected, the High-TiO_2 group displays relatively higher contents of P_2O_5, REE and high field strengh elements (HFSE) elements such as Zr, Ba and Y. The low-TiO_2 group is less evolved or less contaminated as expressed by higher MgO and CaO contents and lower FeO_t contents. The chondrite-normalized REE diagrams (Fig. 7) display enrichment in total content of REE and the negative Eu\Eu* anomalies of the High-TiO2 group. In all tectonic discriminant diagrams (Fig. 8), both groups consistently suggest intraplate continental (CT and E-MORB) to passive margin (E-MORB) environments, with both continental tholeiites and E-MORB signatures. The plosts involving the high-field strength elements, Tb, Ta, Th and Nb (Figs. 8E, 8F) seem to rule out extensional back-arc settings.

On the other hand, as expected, the mafic enclaves included in both the Andrelândia metasedimentary rocks and the orthogranulites of the Juiz de Fora Complex display

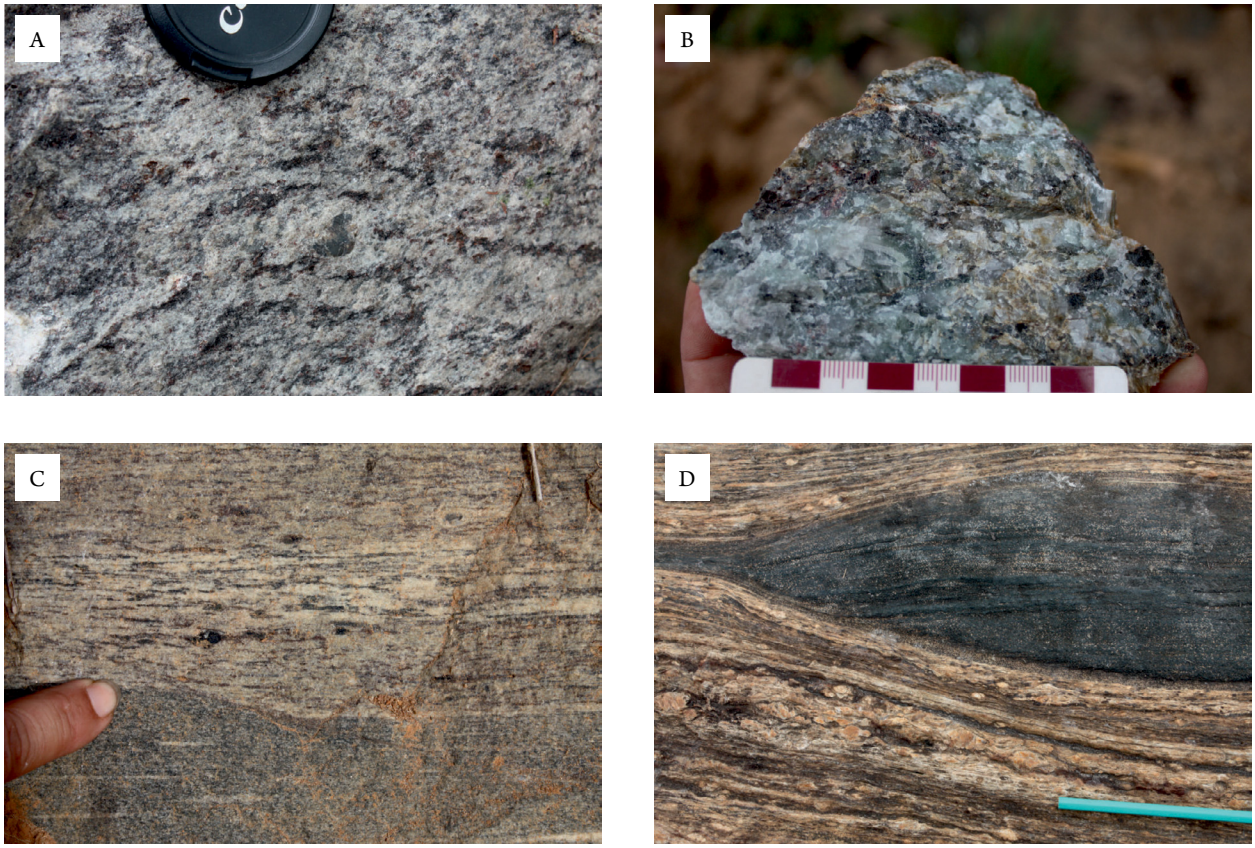

Figure 5. Outcrop images of country rocks of the Barreiro Suite. (A) Garnet-biotite gneiss of the Andrelândia Group; (B) hand sample of Opx-bearing granitoid of the Salvaterra Suite; (C) contact between the leuco-charnockite of the Juiz de Fora Complex and the grey foliated granite of the Bonfim Suite; (D) stretched mafic granulite included in the ortho-granulites of the Juiz de Fora Complex.

heterogeneous geochemical signatures, suggesting different tectonic environments. Using the geochemical data, the enclaves of the country rocks were tentatively separated into four groups (Figs. 7 and 8):

- Group 1 with tholeiitic intraplate signatures, mostly with low-TiO_2 contents, with the exception of a single sample. These enclaves occur both within the orthogranulites of the Juiz de Fora complex and in the metasedimentary rocks of the Andrelândia group. Their geochemical signature is very similar to that obtained from the low-TiO_2 rocks of the Barreiro Suite;
- Group 2 comprises low-TiO_2 samples with E-MORB compositions;
- Group 3 comprises intraplate alkaline mafic rocks, which occur in both the cover and basement associations;
- Group 4 represents the most common signatures for the mafic enclaves within the Juiz de Fora Complex, comprising tholeiitic to calcalkaline compositions (IAT and to

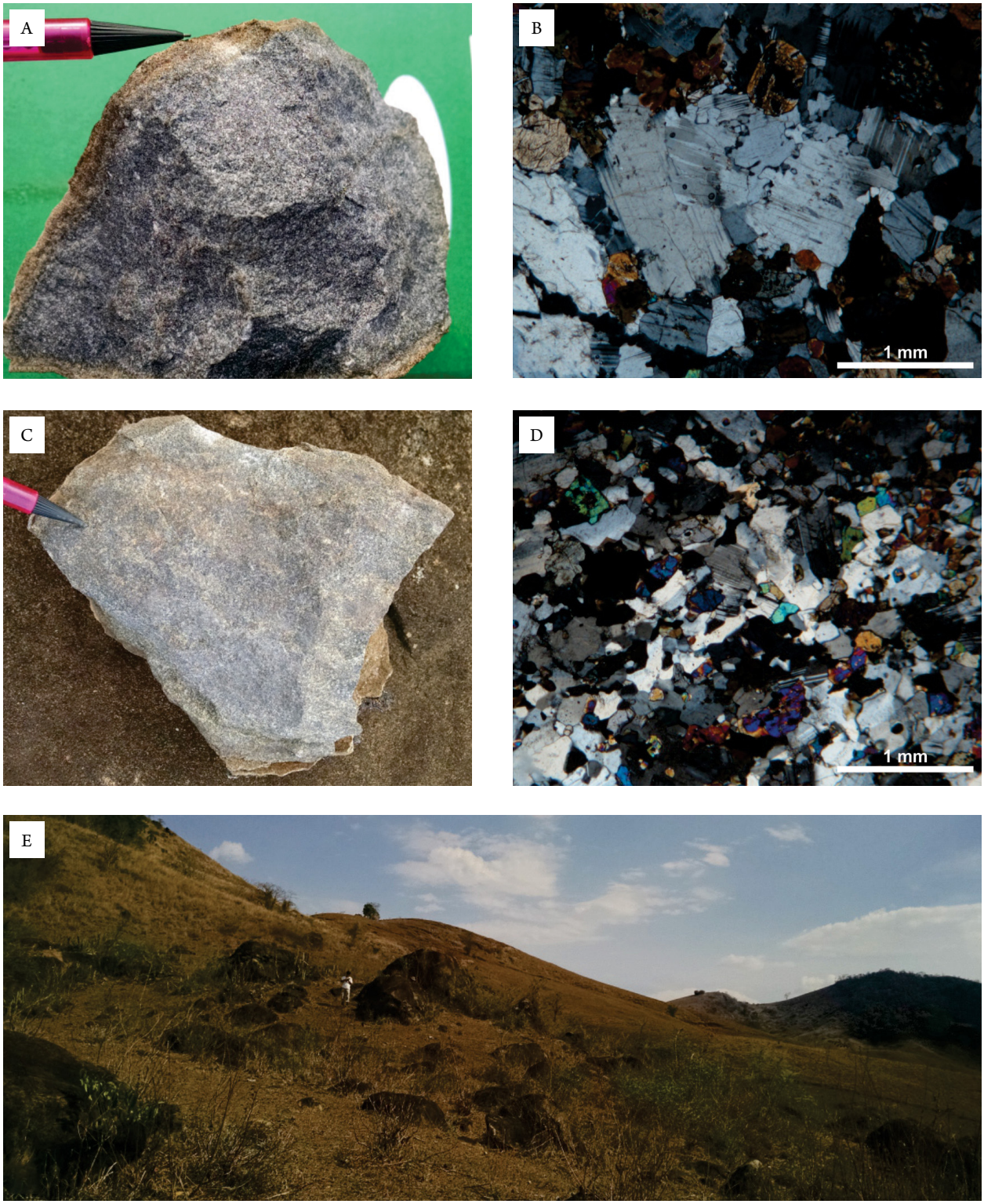

Figure 6. (A) Hand sample and (B) photomicrograph of the coarse-grained variety of metabasic rocks of the Barreiro Suite; (C) hand sample and (D) photomicrograph of the fine-grained variety of the metabasic rocks of the Barreiro Suite; (E) general overview of the Barreiro Suite outcrops with dispersed boulders.

Table 1. Geochemical data of the metabasic rocks

Geochemical Data: Major Elements

Sample	type	Unit	SiO_2	Al_2O_3	FeO	Fe2O3t	MnO	MgO	CaO	Na_2O	K_2O	TiO_2	P_2O_5	LOI	Total
RE-CE-15	$HTiO_2$	BS	53.51	14.66	11.57	12.86	0.274	4.24	9.2	1.65	0.25	2.608	1.35	0.18	100.8
RE-CE-16	$HTiO_2$	BS	52.05	13.95	13.98	15.54	0.313	2.97	7.05	3.41	1.16	3.03	0.91	-0.02	100.4
RE-CE-19	$HTiO_2$	BS	48.74	15.92	12.67	14.08	0.215	5.19	8.19	3.2	0.74	3.117	0.64	0.46	100.5
RE-CE-30B	$HTiO_2$	BS	48.65	15.08	12.2	13.56	0.248	5.96	8.61	2.84	0.6	3.767	1.08	-0.28	100.1
RE-CE-2A	$HTiO_2$	BS	49.19	14.46	12.05	13.39	0.223	4.73	7.92	3.31	0.98	2.437	0.5	1.5	98.65
RE-CE-12	$HTiO_2$	BS	54.48	13.75	12.33	13.7	0.236	2.93	6.66	3.23	1.7	2.815	0.89	-0.1	100.3
RE-CE-13B	$HTiO_2$	BS	51.45	15.6	12.12	13.47	0.267	4.51	7.61	3.48	0.93	2.762	0.63	0.04	100.7
RE-CE-27C	$HTiO_2$	BS	51.02	15.41	12.57	13.97	0.223	3.34	6.75	3.46	2.18	2.832	0.76	0.29	100.2
RE-CE-28C	$HTiO_2$	BS	49.5	17.16	10.53	11.7	0.193	5.91	8.45	3.53	1.11	2.238	0.38	0.54	100.7
RE-CE-29	$HTiO_2$	BS	50.58	16.31	11.23	12.48	0.204	4.82	7.77	3.54	1.46	2.42	0.58	0.46	100.6
RE-CE-30A	$HTiO_2$	BS	50.05	15.32	12.99	14.44	0.225	4.01	7.53	3.09	1.6	3.013	0.78	0.3	100.4
RE-CE-70B	$HTiO_2$	BS	47.98	16.31	13	14.45	0.22	4.84	7.98	3.13	0.71	2.948	0.7	-0.21	99.05
RE-CE-3A	$LTiO_2$	BS	51.81	16.42	9.76	10.85	0.181	5.76	8.56	3.4	0.74	1.919	0.36	0.96	101
RE-CE-03B	$LTiO_2$	BS	48.67	17.22	9.65	10.72	0.188	7.45	9.79	3.03	0.48	1.586	0.28	1.06	100.5
RE-CE-25	$LTiO_2$	BS	51.99	16.83	9.71	10.79	0.174	5.49	7.53	3.59	1.55	1.86	0.33	0.62	100.8
RE-CE-68	$LTiO_2$	BS	57.34	15.8	9.3	10.34	0.157	3.84	6.13	3.39	0.63	1.776	0.41	0.3	100.1
RE-CE-3C	$LTiO_2$	BS	49.41	17.39	9.51	10.57	0.174	6.63	9.3	3.14	0.86	1.679	0.32	0.98	100.4
RE-CE-11	$LTiO_2$	BS	51.24	17.26	9.89	10.99	0.18	5.62	8.69	3.25	0.63	1.764	0.39	0.69	100.7
RE-CE-149	$LTiO_2$	BS	52.7	16.94	10.19	11.32	0.186	6.03	7.76	3.38	0.68	1.724	0.3	-0.07	100.9
MI-BR-39	$LTiO_2$	AND	48	13.88	12.76	14.18	0.21	7.3	11.88	1.41	0.54	1.386	0.1	-0.13	98.75
MI-BE-87B	$LTiO_2$	AND	50.84	15.02	8.9	9.89	0.16	9.57	7.8	2.65	1.87	1.426	0.46	0.67	100.4
PA-BE-133B	$LTiO_2$	AND	49.01	19.04	8.98	9.98	0.156	5.67	8.8	3.47	1.22	1.697	0.29	0.56	99.88
MI-BR-54	$LTiO_2$	JF	40.45	12.52	14.06	15.62	0.301	21.58	6.92	0.51	0.31	0.348	0.09	0.68	99.32
MI-VIII-15	$LTiO_2$	JF	46.8	9.98	9.57	10.64	0.155	21.07	8.98	1.28	0.19	0.335	0.03	1.28	100.7
SP-BR-16	$LTiO_2$	JF	48.84	13.79	13.35	14.84	0.206	6.64	10.85	2.78	0.93	1.435	0.1	0.28	100.7
MI-II-62	$LTiO_2$	JF	49.81	15.24	12.09	13.44	0.172	6.63	9.98	3.22	0.95	0.974	0.14	0.14	100.7
MI-V-40	$LTiO_2$	JF	46.14	14.95	11.12	12.36	0.25	8.31	12.6	2.64	1.17	1.058	0.28	1.04	100.8
MI-BL-27	$LTiO_2$	JF	51.01	14.8	9.37	10.41	0.167	7.58	11.9	1.92	0.65	0.934	0.12	0.88	100.4
PA-BE-146	$LTiO_2$	JF	50.82	13.84	10.88	12.09	0.233	7.76	10.11	2.69	0.71	1.146	0.41	0.11	99.93
PA-BE-136	$LTiO_2$	JF	50.85	15.32	9.75	10.83	0.163	7.41	7.6	3.17	2.39	1.024	0.48	0.09	99.31
SP-BR-06A	$LTiO_2$	JF	50.07	14.36	11.58	12.87	0.185	7.25	8.52	2.82	1.19	0.948	0.23	1.19	99.65
PA-BE-137A	$LTiO_2$	JF	51.27	10.61	10.13	11.26	0.203	12.84	8.85	2.04	2.32	0.629	0.39	0.24	100.7
SP-BR-06C	$LTiO_2$	JF	42.48	18.52	10.95	12.17	0.138	6.24	12.23	2.44	1.44	1.585	1.05	0.99	99.28
SP-BR-17B	$LTiO_2$	JF	49.22	14.16	12.62	14.02	0.187	7.02	11.23	2.33	0.68	1.356	0.11	0.02	100.3
MI-BR-19C	$LTiO_2$	JF	48.56	13.65	13.49	14.99	0.217	6.59	10.03	2.64	1.3	1.557	0.12	0.69	100.3
MI-BR-19E	$LTiO_2$	JF	51.26	14.41	12.26	13.62	0.265	5.4	5.28	2.33	3.35	1.538	0.13	1.35	98.93
PA-BE-92D	$LTiO_2$	JF	44.68	12.52	14.75	16.39	0.247	11.73	8.2	1.56	3.7	0.343	0.04	1.46	100.9
MI-BE-83A	$LTiO_2$	JF	52.16	16.3	9	10.01	0.165	4.99	7.32	3.64	1.42	1.621	0.32	1.2	99.15
MI-IX-03B	$HTiO_2$	JF	51.62	16.41	9.79	10.88	0.156	5.22	7.89	3.15	1.79	2.157	0.86	0.27	100.4
MI-VIII-65	$HTiO_2$	JF	46.78	18.07	9.6	10.67	0.166	4.72	9	3.39	2.57	2.245	1.15	0.57	99.35
MI-III-18	$HTiO_2$	JF	49.11	16.98	11.45	12.72	0.2	5	8.63	3.23	0.68	2.467	0.81	0.07	99.89
MI-BR-56	$HTiO_2$	JF	51.05	16.62	11.4	12.67	0.201	4.03	8.09	3.37	1.48	2.465	1.13	-0.24	100.9

Continue...

Table 1. Continuation

Geochemical Data: Trace Elements																			
Sample	**Type**	**Unit**	**Sc**	**Be**	**V**	**Ba**	**Sr**	**Y**	**Zr**	**Cr**	**Co**	**Ni**	**Cu**	**Zn**	**Ga**	**Ge**	**As**	**Rb**	**Nb**
RE-CE-15	$HTiO_2$	BS	26	5	252	230	593	44	354	200	30	60	20	160	24	2	6	5	29
RE-CE-16	$HTiO_2$	BS	30	2	250	1089	553	49	342	20	34	30	40	180	22	1	< 5	8	28
RE-CE-19	$HTiO_2$	BS	30	1	262	657	610	34	174	30	44	30	40	120	21	1	< 5	3	19
RE-CE-30B	$HTiO_2$	BS	31	1	347	446	569	34	159	70	34	30	30	130	18	1	< 5	7	23
RE-CE-2A	$HTiO_2$	BS	27	2	225	775	507	39	287	20	39	20	30	140	21	2	< 5	8	20
RE-CE-12	$HTiO_2$	BS	28	2	227	1364	528	52	430	< 20	30	< 20	30	170	23	2	< 5	16	28
RE-CE-13B	$HTiO_2$	BS	30	2	211	677	573	40	317	50	38	30	30	130	21	2	< 5	15	20
RE-CE-27C	$HTiO_2$	BS	28	2	224	1605	498	50	545	< 20	31	< 20	30	140	23	1	< 5	24	31
RE-CE-28C	$HTiO_2$	BS	27	2	224	299	556	30	221	40	42	< 20	30	90	20	1	< 5	15	15
RE-CE-29	$HTiO_2$	BS	27	2	229	1147	622	36	573	< 20	38	20	30	110	20	1	< 5	29	19
RE-CE-30A	$HTiO_2$	BS	30	2	261	1377	553	48	510	< 20	36	< 20	30	140	22	1	< 5	13	27
RE-CE-70B	$HTiO_2$	BS	27	2	239	732	619	37	299	< 20	45	< 20	30	140	26	2	< 5	6	20
RE-CE-3A	$LTiO_2$	BS	26	2	207	466	626	20	153	70	37	30	40	100	20	1	< 5	9	12
RE-CE-03B	$LTiO_2$	BS	28	1	180	353	585	23	92	100	42	40	20	80	17	1	< 5	3	9
RE-CE-25	$LTiO_2$	BS	25	2	187	437	537	30	225	40	37	30	30	90	19	1	< 5	67	13
RE-CE-68	$LTiO_2$	BS	23	2	170	372	427	28	152	30	29	< 20	20	100	25	2	< 5	5	18
RE-CE-3C	$LTiO_2$	BS	28	1	212	504	627	29	177	140	37	60	30	80	18	1	< 5	9	11
RE-CE-11	$LTiO_2$	BS	27	2	220	711	646	27	257	30	37	30	30	100	19	1	< 5	5	12
RE-CE-149	$LTiO_2$	BS	24	1	171	427	641	20	81	60	38	40	30	90	21	2	< 5	6	3
MI-BR-39	$LTiO_2$	AND	41	< 1	369	12	146	19	57	150	64	90	30	120	19	2	< 5	7	4
MI-BE-87B	$LTiO_2$	AND	26	2	186	1475	711	26	228	590	44	230	60	90	17	2	< 5	57	14
PA-BE-133B	$LTiO_2$	AND	25	2	189	441	587	24	180	40	35	30	20	60	20	2	< 5	34	3
MI-BR-54	$LTiO_2$	JF	14	< 1	75	327	114	12	13	200	114	450	60	280	9	1	< 5	4	1
MI-VIII-15	$LTiO_2$	JF	33	< 1	186	22	35	19	20	2020	70	870	< 10	50	8	2	< 5	< 2	1
SP-BR-16	$LTiO_2$	JF	39	< 1	392	64	131	31	73	90	56	90	10	120	20	2	< 5	8	4
MI-II-62	$LTiO_2$	JF	36	< 1	253	207	264	20	87	90	49	140	30	110	20	2	< 5	5	4
MI-V-40	$LTiO_2$	JF	45	2	331	399	286	16	94	410	45	90	< 10	120	19	2	< 5	21	3
MI-BL-27	$LTiO_2$	JF	40	< 1	285	181	202	18	80	310	42	90	90	70	17	2	< 5	19	6
PA-BE-146	$LTiO_2$	JF	43	1	170	1164	643	32	102	490	35	110	40	100	18	2	< 5	16	< 1
PA-BE-136	$LTiO_2$	JF	26	2	192	1141	739	22	139	280	35	80	< 10	100	19	2	< 5	55	< 1
SP-BR-06A	$LTiO_2$	JF	47	3	213	165	324	58	188	210	42	100	10	310	23	2	< 5	15	13
PA-BE-137A	$LTiO_2$	JF	30	1	160	880	464	25	146	1000	42	260	< 10	110	15	2	< 5	72	< 1
SP-BR-06C	$LTiO_2$	JF	32	< 1	389	256	765	34	60	30	50	< 20	60	80	22	1	< 5	32	5
SP-BR-17B	$LTiO_2$	JF	40	< 1	358	221	276	21	77	130	67	130	140	130	19	2	< 5	4	4
MI-BR-19C	$LTiO_2$	JF	43	1	419	134	250	30	81	110	54	80	30	150	22	2	< 5	12	10
MI-BR-19E	$LTiO_2$	JF	41	3	200	690	272	83	100	90	40	50	30	190	27	3	< 5	235	47
PA-BE-92D	$LTiO_2$	JF	27	3	180	352	53	23	32	720	54	420	< 10	280	19	2	< 5	157	9
MI-BE-83A	$LTiO_2$	JF	24	2	183	488	494	26	239	< 20	33	20	20	90	19	2	< 5	34	11
MI-IX-03B	$HTiO_2$	JF	19	< 1	237	1070	673	22	148	70	36	60	30	90	18	2	< 5	35	9
MI-VIII-65	$HTiO_2$	JF	28	4	253	1521	1392	39	252	30	15	< 20	10	120	24	2	< 5	75	23
MI-III-18	$HTiO_2$	JF	30	1	266	613	639	36	187	< 20	37	30	30	130	22	2	< 5	9	20
MI-BR-56	$HTiO_2$	JF	29	2	235	1252	674	49	655	40	29	30	30	140	22	2	< 5	16	31

Continue...

Table 1. Continuation

Geochemical Data: Trace and Rare Earth Elements (REE)																				
Sample	**Type**	**Unit**	**La**	**Ce**	**Pr**	**Nd**	**Sm**	**Eu**	**Gd**	**Tb**	**Dy**	**Ho**	**Er**	**Tm**	**Yb**	**Lu**	**Hf**	**Ta**	**Pb**	**Th**	**U**
RE-CE-15	$HTiO_2$	BS	67	142	17.8	75.1	15.3	4.42	12.7	1.8	9.5	1.8	4.9	0.65	4	0.57	7.7	1.6	7	4.5	1.6
RE-CE-16	$HTiO_2$	BS	52.2	114	15.1	65.2	13	3.77	11.5	1.7	9.5	1.8	5.3	0.76	4.8	0.7	6.9	1.5	6	0.8	0.2
RE-CE-19	$HTiO_2$	BS	28.8	64	8.58	36.7	8	2.57	7.3	1.1	6.5	1.3	3.4	0.49	3	0.43	3.7	1	< 5	0.2	< 0.1
RE-CE-30B	$HTiO_2$	BS	36.7	81.8	10.9	44.9	9.1	2.08	7.8	1.1	6.2	1.2	3.1	0.42	2.5	0.38	3.4	1.3	< 5	0.8	0.1
RE-CE-2A	$HTiO_2$	BS	35.3	74.5	9.61	40.5	8.6	2.71	9	1.3	7.4	1.5	4.2	0.58	3.6	0.56	5.9	1	7	0.4	0.2
RE-CE-12	$HTiO_2$	BS	59.2	130	17.1	70.8	14.7	3.66	13.1	1.9	10.8	2.1	5.8	0.79	4.9	0.72	8.9	1.5	7	0.5	0.2
RE-CE-13B	$HTiO_2$	BS	35.8	77.5	10.1	42.8	9.3	2.61	9.1	1.3	7.7	1.5	4.4	0.6	3.7	0.55	6.1	1.1	6	0.6	0.2
RE-CE-27C	$HTiO_2$	BS	59.4	125	16.1	65.4	13	3.8	11.3	1.7	9.7	1.8	5.2	0.72	4.3	0.64	10.1	1.4	9	0.9	0.2
RE-CE-28C	$HTiO_2$	BS	20.1	44.4	5.88	25.6	6.1	2.15	5.6	0.9	5.5	1.1	3.1	0.46	2.9	0.42	4.6	1	< 5	1.2	0.4
RE-CE-29	$HTiO_2$	BS	40.8	84.4	10.5	42	8.4	2.83	7.6	1.1	6.9	1.3	3.8	0.53	3.3	0.5	10.1	1	6	0.8	0.2
RE-CE-30A	$HTiO_2$	BS	53.5	114	14.8	60.2	12.1	3.56	11	1.6	9.2	1.8	4.9	0.7	4.3	0.64	9.7	1.3	8	1	0.2
RE-CE-70B	$HTiO_2$	BS	37.5	81.7	10.8	47.2	10.1	3.1	9.6	1.6	8.6	1.6	4.5	0.67	4	0.59	6.2	1.2	5	0.3	0.1
RE-CE-3A	$LTiO_2$	BS	24.9	50.6	6.51	26.5	5.5	1.83	5.1	0.7	4.3	0.8	2.3	0.33	2.1	0.31	3.4	0.6	6	0.5	0.1
RE-CE-03B	$LTiO_2$	BS	18.1	38.8	5.08	21.5	4.9	1.87	5	0.8	4.4	0.9	2.6	0.36	2.2	0.31	2.3	0.5	< 5	0.5	0.1
RE-CE-25	$LTiO_2$	BS	24.9	50.8	6.53	27	5.8	1.96	6	1	5.9	1.1	3.3	0.46	3	0.44	4.6	0.7	8	2.9	0.8
RE-CE-68	$LTiO_2$	BS	34.9	73.9	9.61	38.5	8	2.02	7.6	1.3	6.8	1.2	3.3	0.51	3	0.38	3.7	1.1	11	4.1	0.9
RE-CE-3C	$LTiO_2$	BS	27.2	60.4	7.89	32.6	7.1	2.01	6.5	1	5.9	1.2	3.3	0.45	2.8	0.41	4	0.5	< 5	0.9	0.2
RE-CE-11	$LTiO_2$	BS	35.2	67.1	8.42	35.1	6.9	2.29	6.6	1	5.4	1.1	3.1	0.43	2.7	0.37	5.5	0.4	7	0.5	0.1
RE-CE-149	$LTiO_2$	BS	17.2	35.8	4.69	20.3	4.2	1.84	4.1	0.7	3.7	0.7	2	0.3	1.9	0.28	1.5	0.7	< 5	0.1	< 0.1
MI-BR-39	$LTiO_2$	AND	6.4	17	2.52	12	3.4	1.13	3.7	0.7	4	0.8	2.3	0.34	2.1	0.34	1.6	0.4	< 5	1.6	0.2
MI-BE-87B	$LTiO_2$	AND	59.4	111	12.7	45.2	7.9	2.07	5.5	0.8	4.5	0.9	2.5	0.38	2.4	0.37	4.1	0.6	9	9.9	1.2
PA-BE-133B	$LTiO_2$	AND	18.4	38	4.87	20.7	4.8	1.61	4.6	0.8	4.6	0.9	2.6	0.41	2.5	0.38	3.6	0.9	< 5	2.3	0.4
MI-BR-54	$LTiO_2$	JF	8.2	5	2.12	8.7	2.1	0.7	2.2	0.4	2.5	0.5	1.3	0.2	1.3	0.21	0.4	0.1	< 5	0.4	0.1
MI-VIII-15	$LTiO_2$	JF	12.1	4.2	3.76	15.9	3.9	1.11	3.3	0.6	3.7	0.7	2	0.31	2	0.28	0.5	< 0.1	< 5	0.4	0.2
SP-BR-16	$LTiO_2$	JF	22.3	16.7	6.05	25.2	6.3	1.99	6.5	1.1	6.6	1.3	3.5	0.5	3.2	0.49	1.9	0.3	< 5	0.4	0.1
MI-II-62	$LTiO_2$	JF	11.7	22.6	3.12	12.8	3.2	0.99	3.7	0.6	3.9	0.8	2.4	0.38	2.4	0.33	2.2	0.3	< 5	0.6	0.1
MI-V-40	$LTiO_2$	JF	15.3	33.6	4.41	18.6	4.3	1.22	3.9	0.6	3.1	0.6	1.8	0.28	1.8	0.25	2	0.3	8	1.2	0.3
MI-BL-27	$LTiO_2$	JF	10	21	2.76	12.1	2.9	0.97	3.1	0.5	3.2	0.6	1.8	0.26	1.7	0.24	1.8	0.3	< 5	1.8	0.4
PA-BE-146	$LTiO_2$	JF	31.9	65.5	8.65	36.9	8	2.25	7.4	1.1	6.4	1.2	3.4	0.51	3	0.44	2.6	0.5	< 5	1.4	0.2
PA-BE-136	$LTiO_2$	JF	23.7	53.3	7.34	31.3	6.7	1.66	5.5	0.8	4.4	0.8	2.4	0.37	2.2	0.3	3.1	0.5	8	0.1	0.1
SP-BR-06A	$LTiO_2$	JF	39	104	15.1	66.5	16	2.26	13.3	2.1	11.2	2	5.4	0.76	4.5	0.68	4.1	0.9	6	2.7	1.6
PA-BE-137A	$LTiO_2$	JF	23.3	56.7	8.08	34.6	7.4	1.59	5.9	0.8	4.5	0.9	2.4	0.4	2.5	0.36	3.1	0.6	< 5	0.3	0.3
SP-BR-06C	$LTiO_2$	JF	22.4	57.8	8.87	42.6	10	2.61	9.2	1.4	7.3	1.4	3.8	0.51	3	0.46	1.9	0.3	< 5	1.7	0.7
SP-BR-17B	$LTiO_2$	JF	5.4	13.2	2.16	10.7	3.2	1.13	3.8	0.7	4.2	0.8	2.4	0.35	2.3	0.37	1.8	0.3	< 5	0.3	< 0.1
MI-BR-19C	$LTiO_2$	JF	24.9	55.9	6.86	25.7	6	1.77	5.9	1.1	6.2	1.2	3.3	0.5	3.2	0.5	2.2	0.7	7	1.1	0.1
MI-BR-19E	$LTiO_2$	JF	53.5	155	23.3	99.4	23.1	2.06	19.1	3.1	17	3.2	8.8	1.34	8.4	1.28	3.1	2.1	12	4.8	0.3
PA-BE-92D	$LTiO_2$	JF	10.3	23.8	3.22	13.2	3.4	1.13	3	0.6	3.6	0.8	2.4	0.39	2.5	0.4	0.9	0.3	< 5	2.5	0.6
MI-BE-83A	$LTiO_2$	JF	27.5	55.7	6.91	28.1	5.9	1.85	5.1	0.8	4.8	0.9	2.6	0.39	2.5	0.37	4.2	0.6	7	1.4	0.3
MI-IX-03B	$HTiO_2$	JF	27.6	60.4	7.96	34.5	6.6	1.89	5.7	0.8	4.3	0.8	2.1	0.3	1.8	0.26	2.7	0.5	< 5	1	0.2
MI-VIII-65	$HTiO_2$	JF	60.8	132	17.3	73.9	14.9	3.52	10.8	1.6	7.7	1.3	3.6	0.52	3.1	0.42	4.9	1.1	8	4.2	1
MI-III-18	$HTiO_2$	JF	33.2	76	10.3	45.7	9.4	2.51	7.9	1.2	6.9	1.3	3.5	0.56	3.3	0.44	3.5	0.9	< 5	0.3	< 0.1
MI-BR-56	$HTiO_2$	JF	62.6	139	18.8	76.6	15.2	3.02	12.6	1.8	9.6	1.7	4.8	0.73	4.5	0.63	11.8	1.2	8	0.9	0.1

CAB), indicating arc-related environments. As mafic rocks of this group crop out only within the orthogranulites of the Juiz de Fora complex, we suggest that they belong to the convergent Rhyacian history of the basement.

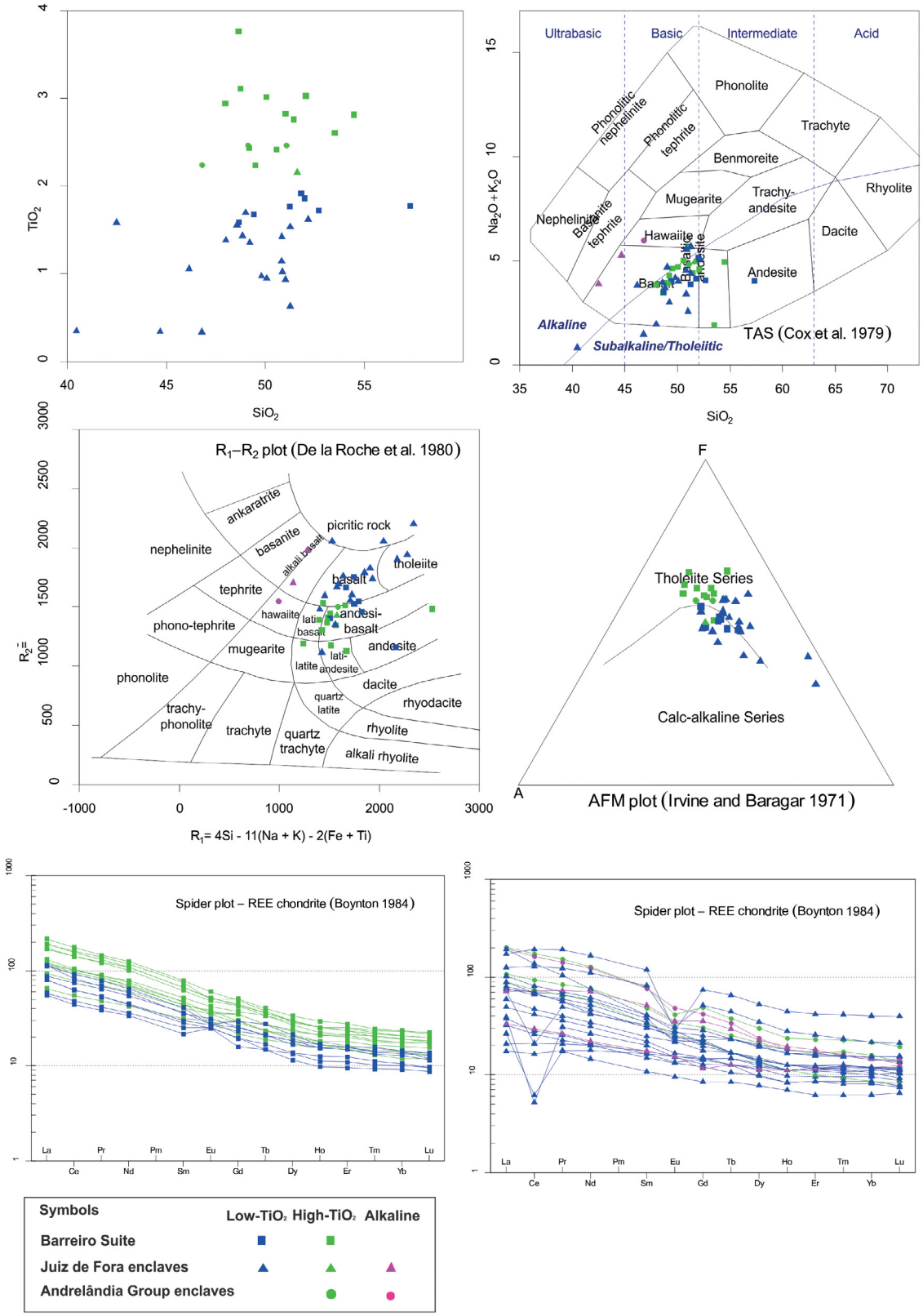

Figure 7. Geochemical data for the rocks of the Barreiro Suite and mafic enclaves within the country rocks: (A) binary $TiO_2 \times SiO_2$ diagram with subdivision into two groups; (B) chemical classification of the analysed rocks in the TAS diagram of Cox *et al.* (1989); (C) chemical classification in the R1 × R2 diagram of De La Roche *et al.* (1980); (D) AFM diagram of Irvine and Baragar (1971); (E) chrondrite-normalized spidergram of the High-TiO_2 and Low-TiO_2 groups of the Barreiro Suite; (F) chrondrite-normalized spidergram including alkaline basic enclaves in the Andrelândia Group and Juiz de Fora Complex. Both spidergrams were normalized using the chondrite composition of Boynton (1984).

Enclaves of groups 1 to 3 (both Andrelândia Group and Juiz de Fora Complex) and all Barreiro Suite samples plot in the intraplate to passive margin extensional settings (Fig. 8). On the other hand, the Group 4 of the Juiz de Fora Complex (CAB to IAT convergent tectonic settings) is probably related with the Rhyacian history of the basement (Fig. 8).

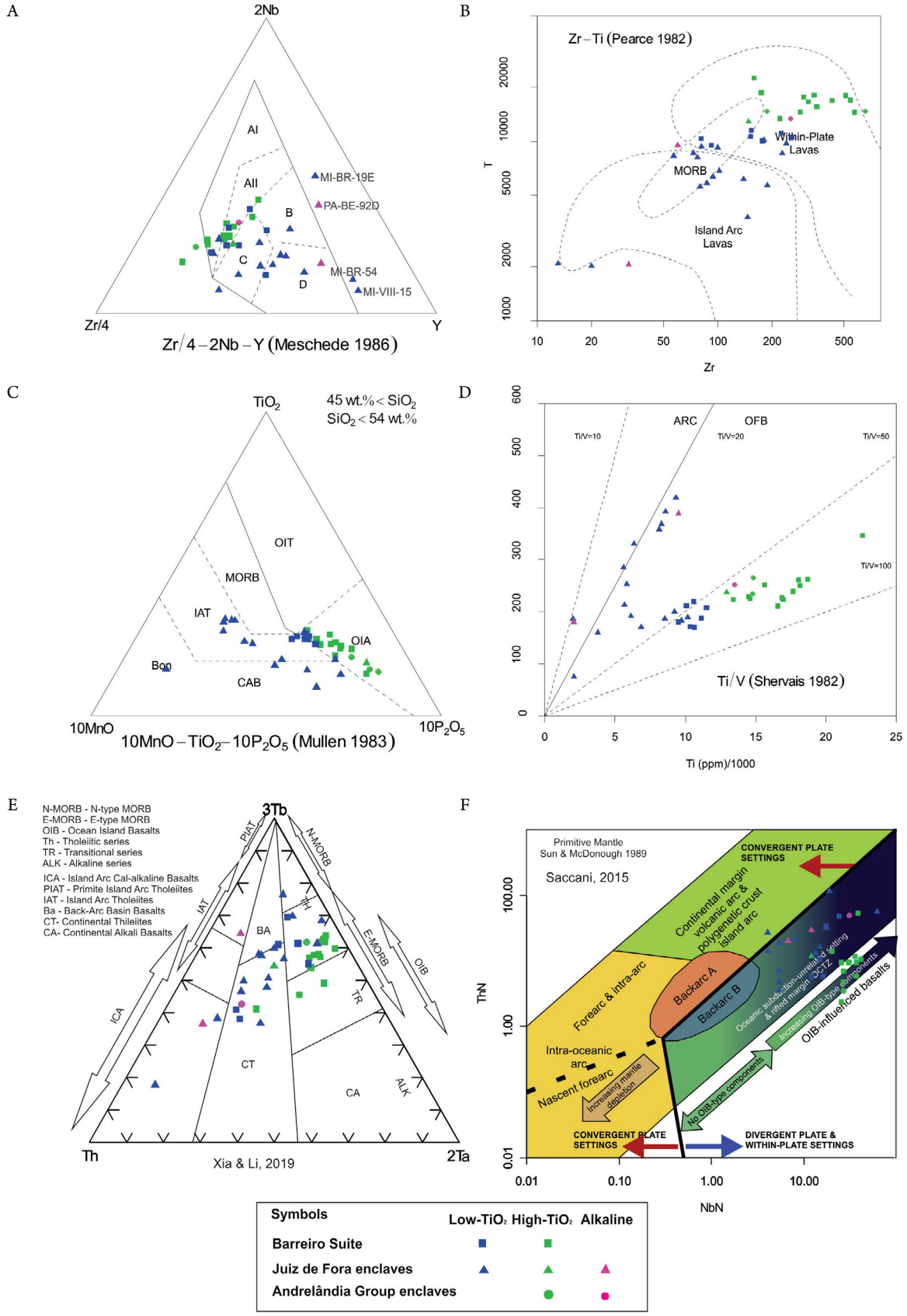

Figure 8. Plot of analyzed sample in tectonic diagrams: (A) Zr/4- 2Nb-Y triangular diagram of Meschede (1986); (B) Zi × Ti of Pearce (1982); (C) TiO2 x 10 MnO × 10 P2O5 triangular diagram of Mullen (1983); and (D) Ti x V diagram of Shervais (1982), (E) triangular diagram of Cabanis and Thiéblemont (1988), in Xia and Li (2019); (F) normalized binary diagram of Scanni (2015) (normalized by Sun & McDonough 1989)

U-PB GEOCHRONOLOGY AND HF ISOTOPES OF THE BARREIRO SUITE

In order to constrain the age of the intraplate magmatism of the Barreiro Suite, sample MI-BR-68, a diorite, was selected for U-Pb analysis. This sample produced the largest number of recovered zircons suitable for geochronological investigation.

Preparation and analytical procedures

The sample preparation involved crushing (ca. 30 kg) and manual panning, followed by density and magnetic separation in the LGPA laboratory of the UERJ. Zircons typically show pale brown to pink colors, with short prismatic habit (2:1 to 3:1 aspect ratios), and less commonly with sub-equant shapes. Scanning electron microscope cathodoluminescence images were obtained at the MULTILAB facilities of the UERJ. Most of the grains display complex zoning patterns, rounded bright overgrowths and resorption textures that, with typical soccer ball grains, are typical of high-grade metamorphism (Rubatto 2017).

U-Pb isotopic data were obtained at the Geochronology Laboratory of the Universidade de Brasília (UnB) using a Thermo-Finnigan Neptune multicollector inductively coupled plasma mass spectrometer connected to a "New Wave 213 mm Nd-YAG" laser beam with spot diameters of 30 to 50 μm, and frequency of 6 to 10 Hz. Bracketing technique of analyses, described in detail by Bühn *et al.* (2009), involved the use of the JG1, Temora 2 and FC1 standards. For the standard and sample analyses, isotope ratio measurements consist of blocks of 40 cycles, each with 1.049 sec duration.

Analyses with either errors higher than 10% for isotope ratios, ^{204}Pb contents higher than 0.5%, or discordance above 5%, were not considered in the age calculations. Analyses with ^{206}Pb/^{204}Pb ratios higher than 3,000 indicate negligible common Pb contents, obviating the need for common Pb correction. When necessary, the correction is made with the in-house spreadsheet of Bühn *et al.* (2009), following Stacey and Kramers (1975). Age calculations and plots were performed with the Isoplot V.3 software of Ludwig (2003).

The Lu-Hf analyses were performed at the University of Notre Dame (USA), using a UP193 nm laser ablation system coupled to a NuPlasma II Multi-Collector ICPMS. The Lu-Hf spots were located as the same zircon texture domains of the U-Pb spots. Analytical conditions were laser spots of 50 μm diameter, 60 s of ablation after a run of 30 s for background, pulse of 5 Hz corresponding to an energy fluence of ~10 J/cm^2. Methodology followed the protocol of Simonetti and Neal (2010), using the Plesovice, BR266 and 1500 standards. Mass interference of ^{176}Lu with ^{176}Hf was corrected using the ^{176}Lu/^{175}Lu ratio of 0.02655 (International Union of Pure and Applied Chemistry 1998), and the decay constant of ^{176}Lu of 867×10^{-11} (Söderlund *et al.* 2004). Chondritic ratios used for ε_{Hf} calculations were ^{176}Hf/^{177}Hf = 279718, ^{176}Lu/^{177}Hf = 0.0336 (Bouvier *et al.* 2008), and present-day depleted mantle ratios of ^{176}Hf/^{177}Hf = 0.28325 and ^{176}Lu/^{177}Hf = 0.0388 (Griffin *et al.* 2000; updated by Andersen *et al.* 2009).

U-Pb results

Analysis of sample MI-BR-68 produced 45 spots (Tab. 2), nine of which were discarded due to poor analytical parameters such as isotope ratios errors higher than 10%, ^{204}Pb contents higher than 0.5%, or discordance above 5%.

All zircons plot along the Concordia between ca. 780 Ma and ca. 610 Ma (Fig. 9), perhaps suggesting ion diffusion under high-temperatures of the regional granulite facies metamorphism. It also confuses distinction between igneous and metamorphic zirons on the basis of zircon textures and Th/U (Rubatto 2017). However, based on the bimodal pattern of the probability density plot of 207 Pb/206 Pb ages (Fig. 9), a group of 8 zircons with concentric oscillatory zoning and relatively high Th/U ratios (Rubatto 2017) yielded a Concordia age of 766 ± 13 Ma, interpreted as the age of reference for the mafic magmatism. The cluster of younger zircons, with relatively lower Th/U ratios, yielded a Concordia age of 619 ± 6 Ma, interpreted as the best estimate for the age of the metamorphic overprint. This latter age is comparable with the early metamorphic ages reported for the Ribeira Belt (Bento dos Santos *et al.* 2007, Machado *et al.* 1996, Heilbron & Machado 2003). Field observations support this interpretation, such as the presence of thin leucocratic intrusive veins and partial digestion of the mafic enclaves of the Barreiro Suite within the syn-collisional granitoid rocks.

Three inherited zircons, with ages of ca. 1.38 Ga, 2.14 Ga and 2.15 Ga, reflect the basement associations of the Occidental terrane of the Ribeira Belt, confirming the intraplate setting of the Barreiro Suite as indicated by geochemical criteria.

Lu-Hf results

Lu-Hf analyses (Tab. 3) were performed on the same sample as the U-Pb analyses. Zircon grains were selected for the investigation of crystallization age, metamorphic overprint and inheritance. Measured ^{176}Hf/^{177}Hf ratios vary between 0.281927 and 0.282559, while ^{176}Lu/^{177}Hf ratios are below 0.0015.

Zircons with late Tonian ages, interpreted as crystallization ages, yield a broad spectrum of T_{DM} Hf model ages, as expected for intraplate basaltic rocks, ranging from ca. 1.75 to 0.96 Ga with predominantly positive $\varepsilon Hf_{(t = 766)}$ values between + 5.61 and + 0.24. Two grains yielded negatives $\varepsilon Hf_{(t = 766)}$ values of -10.97 and of -4.07 (Fig. 10).

On the other hand, most of the Ediacaran metamorphic zircons and overgrowths, with U-Pb ages between 624 and 594 Ma, yielded Hf T_{DM} model ages between 1.80 Ga and 1.04 Ga, with negative $\varepsilon Hf_{(t = 766)}$ values between -10.86 and -1.82. The metamorphic zircons are interpreted as having grown from *in situ* melting films within the basic rocks, the preservation of primary ^{176}Hf/^{177}Hf compositions in metamorphic zircon can be usually attributed to subsolidus recrystallization (Zeh *et al.* 2010), as strongly suggested by very complex textures detected on the cathodoluminescence images. Tedeschi *et al.* (2018) obtained similar results for high-temperature granulites in the Southern Brasília belt.

The single grain with age of ca. 1.39 Ga represents inheritance, with a Hf T_{DM} model age of 1.62 Ga with $\varepsilon Hf_{(t = 1.62)}$ of +5.61, suggesting juvenile sources.

Table 2. Summary of U-Pb zircon data obtained by inductively coupled plasma mass spectrometry (LA-ICPMS) (Mi-BR-68) - ZIRCON

Spot/	Th ppm	U ppm	Pb ppm	Th/U	f-206	Ratios						Age (Ma)						Discordance %
						$^{207}Pb^*/^{235}U$	1σ	$^{206}Pb^*/^{238}U$	1σ	Rho	$^{207}Pb^*/^{206}Pb^*$	1σ	$^{206}Pb/^{238}U$	1σ	$^{207}Pb/^{235}U$	1σ	$^{207}Pb/^{206}Pb$	1σ	
Z-01	176	360	41	0.49	0.0009	0.81869	3.63	0.09884	3.10	0.85	0.06008	1.89	608	19	607	22	606	11	0
Z-02	132	96	14	1.38	0.0031	1.03905	4.70	0.12048	2.83	0.60	0.06255	3.75	733	21	723	34	693	26	-6
Z-03	71	298	41	0.24	0.0007	1.17151	2.42	0.13013	1.77	0.73	0.06529	1.66	789	14	787	19	784	13	-1
Z-04	150	350	39	0.43	0.0010	0.88157	2.65	0.10567	1.98	0.75	0.06051	1.77	648	13	642	17	622	11	-4
Z-05	57	77	10	0.75	0.0027	0.81597	5.96	0.09855	4.61	0.77	0.06005	3.77	606	28	606	36	605	23	0
Z-06	200	346	38	0.58	0.0007	0.81093	3.33	0.09780	2.82	0.85	0.06014	1.77	602	17	603	20	608	11	1
Z-07	12	66	17	0.18	0.0019	2.91376	2.67	0.23946	2.16	0.81	0.08825	1.56	1384	30	1385	37	1388	22	0
Z-08	45	333	44	0.14	0.0006	1.17653	2.83	0.13035	2.33	0.82	0.06546	1.60	790	18	790	22	789	13	0
Z-09	41	687	70	0.06	0.0005	0.79912	3.71	0.09649	3.35	0.90	0.06007	1.58	594	20	596	22	606	10	2
Z-10	66	155	18	0.43	0.0018	0.85099	4.27	0.10161	3.17	0.74	0.06074	2.86	624	20	625	27	630	18	1
Z-11	22	1005	96	0.02	0.0003	0.78038	3.72	0.09518	3.34	0.90	0.05947	1.64	586	20	586	22	584	10	0
Z-12	26	168	21	0.16	0.0012	1.07514	3.36	0.12121	2.42	0.72	0.06433	2.33	738	18	741	25	753	18	2
Z-13	25	40	8	0.63	0.0026	0.84299	6.07	0.10107	4.51	0.74	0.06049	4.06	621	28	621	38	621	25	0
Z-14	30	46	8	0.65	0.0048	1.18654	6.45	0.13132	4.74	0.73	0.06553	4.38	795	38	794	51	791	35	0
Z-15	140	217	24	0.65	0.0012	0.80498	3.64	0.09731	2.91	0.80	0.06000	2.18	599	17	600	22	603	13	1
Z-16	52	276	30	0.19	0.0010	0.81484	4.23	0.09851	3.84	0.91	0.05999	1.77	606	23	605	26	603	11	0
Z-17	79	351	38	0.23	0.0010	0.81989	3.67	0.09884	3.24	0.88	0.06016	1.73	608	20	608	22	609	11	0
Z-18	14	331	32	0.04	0.0015	0.82274	3.71	0.09891	3.24	0.87	0.06033	1.80	608	20	610	23	615	11	1
Z-19	39	69	8	0.58	0.0025	0.82829	7.43	0.09977	5.68	0.76	0.06021	4.78	613	35	613	45	611	29	0
Z-20	82	62	9	1.33	0.0044	1.16436	5.89	0.12907	4.55	0.77	0.06543	3.75	783	36	784	46	788	30	1
Z-21	67	455	42	0.15	0.0009	0.91080	2.90	0.10738	2.25	0.78	0.06152	1.83	658	15	657	19	657	12	0
Z-22	56	173	16	0.33	0.0023	0.81295	4.73	0.09820	3.68	0.78	0.06004	2.96	604	22	604	29	605	18	0
Z-23	45	297	26	0.15	0.0012	0.81363	3.83	0.09815	3.04	0.79	0.06013	2.33	604	18	604	23	608	14	1
Z-24	51	92	12	0.55	0.0025	1.03636	7.44	0.11878	6.17	0.83	0.06328	4.15	724	45	722	54	718	30	-1
Z-25	**2**	**28**	**2**	**0.08**	**0.0119**	**0.72127**	**19.74**	**0.08933**	**14.3**	**0.72**	**0.05856**	**13.7**	**552**	**79**	**551**	**109**	**551**	**75**	**0**
Z-26	151	183	70	0.83	0.0004	7.44485	1.85	0.39657	1.39	0.76	0.13616	1.21	2153	30	2166	40	2179	26	1
Z-27	9	17	6	0.51	0.0023	7.24563	6.67	0.39303	4.15	0.62	0.13370	5.23	2137	89	2142	143	2147	112	0
Z-28	44	156	15	0.29	0.0024	0.94416	4.48	0.11023	3.69	0.82	0.06212	2.55	674	25	675	30	678	17	1
Z-29	69	115	12	0.60	0.0026	0.89659	5.08	0.10611	3.70	0.73	0.06128	3.49	650	24	650	33	649	23	0
Z-30	44	338	30	0.13	0.0009	0.81589	3.90	0.09824	3.41	0.88	0.06023	1.89	604	21	606	24	612	12	1
Z-31	29	121	9	0.25	0.0016	0.84257	5.18	0.10108	3.44	0.66	0.06046	3.87	621	21	621	32	620	24	0
Z-32	21	99	9	0.22	0.0024	1.08145	5.02	0.12212	3.27	0.65	0.06423	3.81	743	24	744	37	749	29	1
Z-33	60	166	14	0.36	0.0018	0.83414	4.90	0.10011	4.31	0.88	0.06043	2.33	615	26	616	30	619	14	1
Z-34	45	241	20	0.19	0.0008	0.84907	4.00	0.10167	3.26	0.82	0.06057	2.31	624	20	624	25	624	14	0
Z-35	57	263	24	0.22	0.0014	0.83449	3.34	0.10021	2.76	0.83	0.06039	1.88	616	17	616	21	618	12	0
Z-36	7	627	51	0.01	0.0005	0.83278	3.30	0.10023	2.81	0.85	0.06026	1.72	616	17	615	20	613	11	0
Z-37	29	87	8	0.34	0.0030	0.83633	6.24	0.10043	5.03	0.81	0.06040	3.69	617	31	617	38	618	23	0
Z-38	262	202	28	1.30	0.0013	0.92605	3.73	0.10856	3.04	0.81	0.06187	2.17	664	20	666	25	670	15	1
Z-39	79	140	16	0.57	0.0018	0.82444	4.94	0.09918	4.02	0.81	0.06029	2.87	610	24	611	30	614	18	1
Z-40	60	178	19	0.34	0.0021	0.82405	3.89	0.09920	2.92	0.75	0.06025	2.56	610	18	610	24	613	16	0
Z-41	19	95	11	0.21	0.0032	0.87459	5.18	0.10374	4.08	0.79	0.06114	3.19	636	26	638	33	644	21	1
Z-42	180	326	31	0.56	0.0008	0.83788	2.81	0.10108	2.38	0.85	0.06012	1.50	621	15	618	17	608	9	-2
Z-43	44	138	13	0.32	0.0018	0.83850	4.82	0.10095	3.57	0.74	0.06024	3.24	620	22	618	30	612	20	-1
Z-44	369	312	39	1.19	0.0011	0.83308	2.67	0.09968	2.24	0.84	0.06062	1.45	613	14	615	16	626	9	2
Z-45	236	542	56	0.44	0.0009	0.87582	2.55	0.10566	2.07	0.81	0.06012	1.48	647	13	639	16	608	9	-7

[1]Sample and standard are corrected after Pb and Hg blanks; [2]$^{207}Pb/^{206}Pb$ and $^{206}Pb/^{238}U$ are corrected after common Pb presence. Common Pb assuming $^{206}Pb/^{238}U$ - $^{207}Pb/^{235}U$ concordant age; [3]f-206 denotes the percentage of ^{206}Pb that is common Pb; [4]$^{235}U = 1/137.88*Utotal$; [5]Standard GJ-1; [6]$Th/U = {}^{232}Th/{}^{238}U$ *0.992743; [7]All errors in the table are calculated 1 sigma (% for isotope ratios, absolute for ages) samples marked in bold letters are discarded.

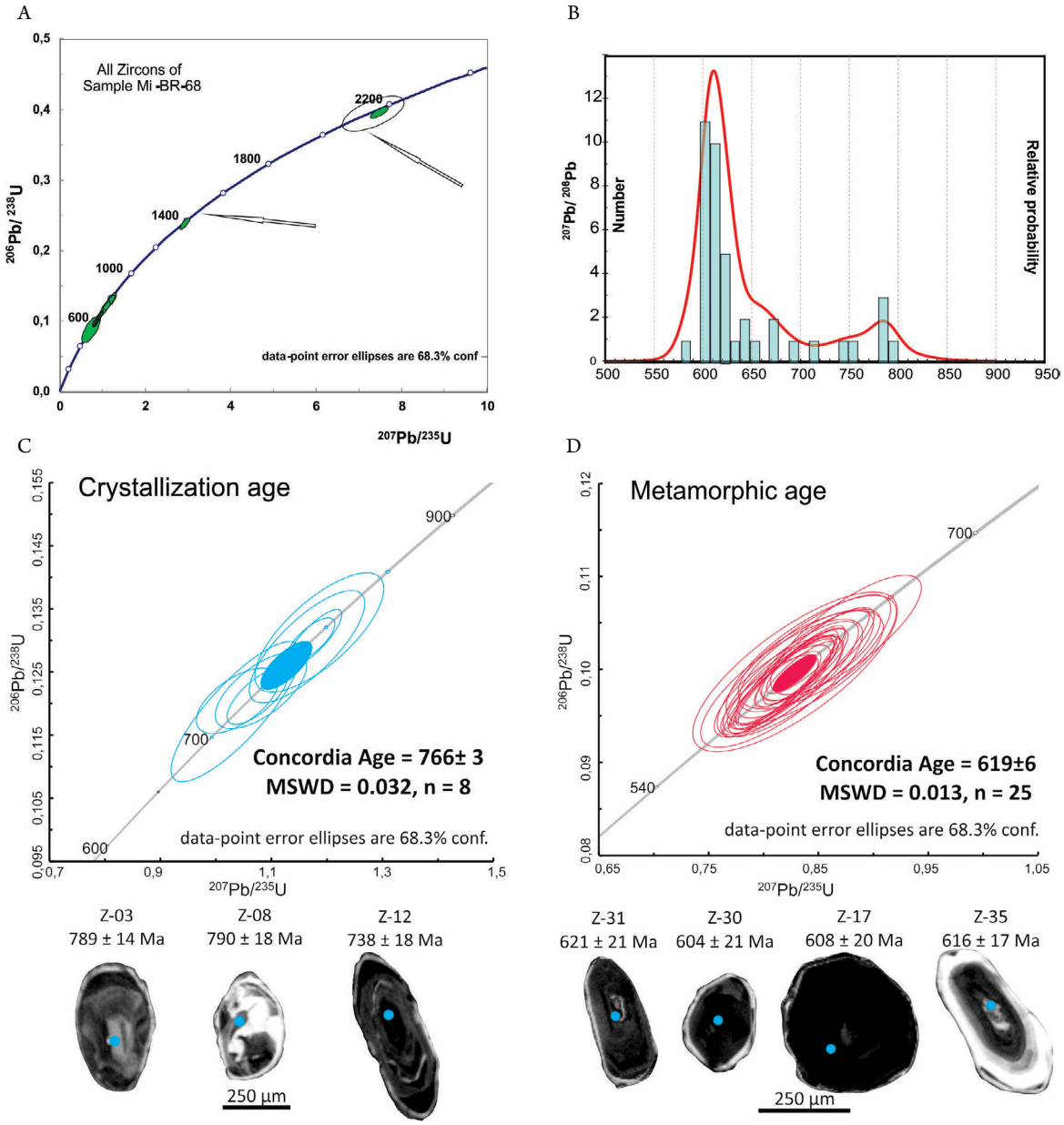

Figure 9. LA_ICPMS U-Pb data for sample MI-BR-68 of the Barreiro Suite. (A) Concordia diagram for all analysed zircons, indicating the Mesoproterozoic and Paleoproterozoic inheritance; (B) relative probability plot of $^{207}Pb/^{206}Pb$ ages showing the bimodal pattern; (C) calculated crystallization age of 766 ± 3 Ma with selected images of analysed zircons; (D) calculated high-grade metamorphic overprint age of 619 ± 6 Ma.

Table 3. Lu-Hf data of sample MI-BR-68

Sample	U-Pb age (Ma)	Sample (present-day ratios)			Sample (initial ratios)			T DM (Ma)
		$^{176}Hf/^{177}Hf$	±2SE	$^{176}Lu/^{177}Hf$	$^{176}Hf/^{177}Hf$ (t)	eHf(t)	±2SE	
MI-BR-68_01(z36)	616	0,281927	0,000018	0,000018	0,281927	-16,62	0,47	1796
MI-BR-68_02(z37)	617	0,282125	0,000021	0,000165	0,282123	-9,66	0,49	1538
MI-BR-68_03(z16)	606	0,282354	0,000014	0,000237	0,282351	-1,83	0,07	1230
MI-BR-68_04(z19)	613	0,282402	0,000013	0,000499	0,282397	-0,06	0,00	1172
MI-BR-68_05(z17)	608	0,282294	0,000014	0,000028	0,282294	-3,82	0,12	1305
MI-BR-68_06(z03)	789	0,282328	0,000014	0,001451	0,282306	0,69	0,01	1307
MI-BR-68_07(z20)	783	0,282338	0,000016	0,001000	0,282323	1,17	0,05	1277
MI-BR-68_08(z14)	795	0,281983	0,000015	0,000702	0,281972	-10,98	0,52	1752
MI-BR-68_09(z12)	738	0,282218	0,000014	0,000977	0,282204	-4,08	0,10	1442
MI-BR-68_10(z15)	599	0,282497	0,000015	0,000411	0,282493	3,02	0,09	1040
MI-BR-68_11(z10)	624	0,282496	0,000014	0,000389	0,282491	3,53	0,11	1042
MI-BR-68_12(z07)	1388	0,282066	0,000014	0,000165	0,282061	5,62	0,09	1617
MI-BR-68_15(z28)	733	0,282558	0,000018	0,000664	0,282548	8,02	0,23	964
MI-BR-68_16(z42)	621	0,282335	0,000015	0,000108	0,282334	-2,10	0,05	1252
MI-BR-68_18(z22)	604	0,282425	0,000017	0,000332	0,282422	0,62	0,02	1136
MI-BR-68_21(z09)	594	0,282105	0,000013	0,000090	0,282103	-10,86	0,37	1562
MI-BR-68_22(z31)	621	0,282146	0,000015	0,000053	0,282146	-8,77	0,30	1504

Sm-Nd AND Sr ISOTOPES

Analytical procedures

Thirteen samples of the Barreiro suite and from mafic enclaves within Juiz de Fora Complex and Andrelândia Group country rocks were selected. Samples preparation involved fragmentation with a jaw crusher and milling at the LGPA-UERJ.

Sm-Nd and Sr isotopic data were obtained by at the Laboratory Geochronology and Radiogenic Isotopes (LAGIR) of the UERJ, where chemical procedures are carried out in clean rooms using purification of Milli-Q® water and PA Merck® acids purified by repeated sub-boiling distillation. Between 25 and 50 mg of pulverized rock samples were subjected to digestion in Savillex® vessels on a hot plate, after the addition of proportional amounts of a double ^{149}Sm-^{150}Nd tracer, using a mixture of concentrated HF and HNO_3 6N for 3 days, followed by further digestion with HCl 6N for 2 days. Separation of Sr and REE used cation exchange following conventional techniques with Teflon columns filled with Biorad AG50W-X8 resin (100–200 mesh) in HCl medium. For the separation of Sm and Nd from the other REE, a secondary column was used with the Eichrom LN-B-25S (50–100 μm) resin.

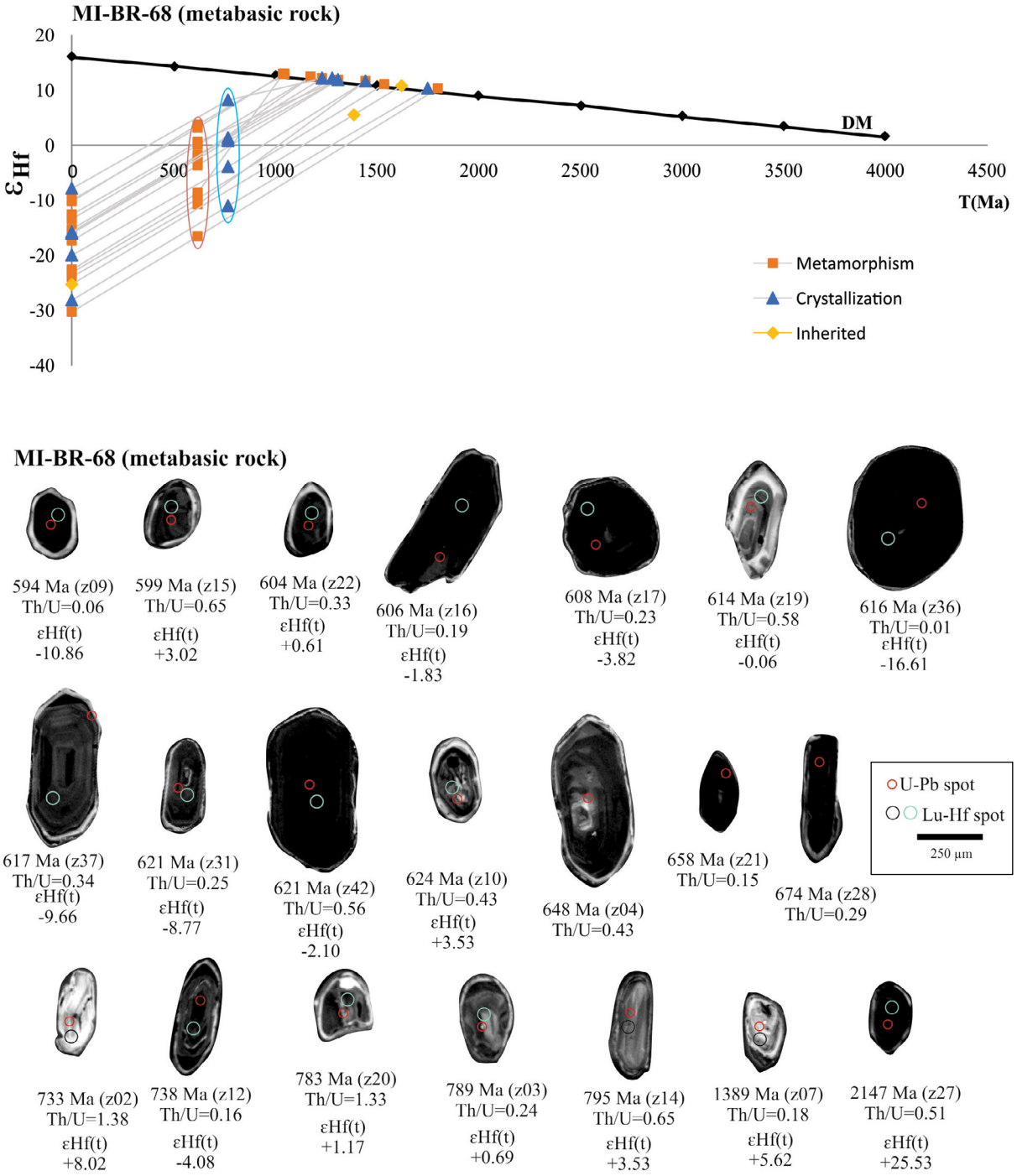

Figure 10. Hf evolution diagram for the analysed zircons. The blue ellipse highlights data for zircons defining the crystallization age, while the red ellipse shows the data for metamorphic zircons. A single datum for the Mesoproterozoic inherited zircon grain is presented in yellow. Selected images with both the U-Pb and Lu-Hf targets and Th-U ratios are presented below. As expected for high-grade metamorphism the analysed zircons do not have low Th/U ratios.

After evaporation Sm, Nd and Sr samples were separately loaded onto previously degassed Re filaments assembled in double filament mounts, using H3PO4 as ionization activator.

Isotope ratios were measured with a Thermo Scientific TRITON in static mode using up to 8 Faraday collectors. The measured isotope ratios are reported with absolute standard errors (2σ) below 0.00001. The measured ratios were normalized respectively to the natural constant ratios of $^{146}Nd/^{144}Nd = 0.7219$, $^{147}Sm/^{152}Sm = 0.5608$ and $^{88}Sr/^{86}Sr = 8.3762$. The average $^{143}Nd/^{144}Nd$ ratio of repeated measurements of the JNdi-1 reference material (Tanaka *et al.* 2000) is 0.512098 ± 0.000006 (n = 322). The average $^{87}Sr/^{86}Sr$ ratio of the NBS-987 reference material (Wise & Waters 2007) is 0.710239 ± 0.000007 (n=158). Repeated analyses of the BCR and AVG rock reference materials from the United States Geologic Survey yield $^{147}Sm/^{144}Nd$ ratios with reproducibility within 1% (Valeriano *et al.* 2008). Neodymium (T_{DM}) model ages were calculated using the depleted mantle model of De Paolo (1981).

Sm-Nd and Sr isotopes results

The location of samples is shown in Figures 3 and 4, and the analytical results are presented in Table 4. Two isotopic groups can be discriminated. The majority of samples, including all those from the Barreiro suite, part of those from the Juiz de Fora Complex, and one single sample occurring within the metasedimentary rocks of Andrelândia-Raposos group yielded late Paleoproterozoic to Mesoproterozoic T_{DM} model ages, between ca. 1.80 Ga and 1.50 Ga. The εNd_t values obtained are -8 to -3, and initial $^{87}Sr/^{86}Sr$ ratios between 0.7017 and 0.7092. This range of values suggests different degrees of contamination from country rocks, as indicated by inherited zircons with old U-Pb ages.

Sample RE-CM-28C, with highest Mg number, shows less contaminated isotopic signatures, probably reflecting the primary composition of the mafic magma with low SiO_2 and high MgO contents. The young T_{DM} age of 0.97 Ga, ε_{t} = +4.1 and initial $^{87}Sr/^{86}Sr$ 0.7036 of this sample characterize it as the most primitive sample of the Barreiro Suite (Fig. 11).

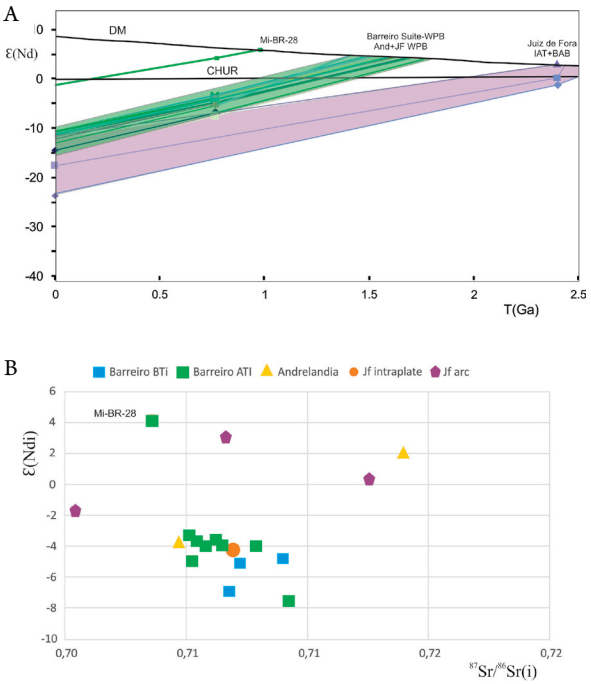

Figure 11. Sm-Nd isotopic data for selected analysed samples. (A) Nd evolution diagram; (B) $\varepsilon nd_{(i)} \times {}^{87}Sr/^{86}Sr_{(i)}$ diagram for the samples of Barreiro Suite and a few mafic enclaves from the Andrelândia Group and Juiz de Fora Complex.

Table 4. Sm-Nd and Sr isotopic data of the metabasic rocks

Sample	Unit	Sm ppm	Nd ppm	Rb* ppm	Sr ppm	$^{143}Nd/^{144}Nd$	abs st error	$^{147}Sm/^{144}Nd$	$^{87}Sr/^{86}Sr$	abs st error	t (Ma)	ε 0 Ma	f (Sm/Nd)	$^{143}Nd/^{144}Nd_{(t)}$	ε (t)	T_{DM} Ga	$^{87}Sr/^{86}Sr_{(t)}$
RE-CE-03A	Barreiro LTi	6.2	31.1	9	626	0.511899	0.000005	0.1200	0.707183	0.000006	766	-14.4	-0.38972	0.511296	-6.9	1.76	0.7067
RE-CE-149	Barreiro LTi	4.6	21.5	6	641	0.512056	0.000008	0.1296	0.709232	0.000008	766	-11.4	-0.34095	0.511405	-4.8	1.69	0.7089
RE-BR-68	Barreiro LTi	8.1	39.2	5	427	0.512018	0.000007	0.1257	0.707539	0.000004	766	-12.1	-0.36087	0.511387	-5.1	1.68	0.7072
RE-CE-2A	Barreiro HTi	9.9	46.6	8	507	0.512094	0.000005	0.1286	0.706950	0.000009	766	-10.6	-0.34611	0.511448	-4.0	1.61	0.7065
RE-CE-13B	Barreiro HTi	10.4	48.7	15	573	0.512049	0.000004	0.1288	0.706041	0.000005	766	-11.5	-0.34529	0.511402	-4.9	1.68	0.7052
RE-CE-28C	Barreiro HTi	5.7	24.4	15	556	0.512569	0.000004	0.1406	0.704435	0.000010	766	-1.4	-0.28519	0.511862	4.1	0.97	0.7036
RE-CE-29	Barreiro HTi	9.3	46.7	29	622	0.512088	0.000006	0.1209	0.706583	0.000007	766	-10.7	-0.38529	0.511481	-3.3	1.50	0.7051
RE-CE-30A	Barreiro HTi	8.3	41.7	13	553	0.512048	0.000006	0.1205	0.708587	0.000007	766	-11.5	-0.38746	0.511443	-4.1	1.55	0.7078
RE-CE-30B	Barreiro HTi	10.5	53.5	7	569	0.511861	0.000005	0.1188	0.709596	0.000004	766	-15.2	-0.39591	0.511264	-7.6	1.80	0.7092
RE-CE-70B	Barreiro HTi	10.0	47.9	6	619	0.512091	0.000003	0.1267	0.705819	0.000009	766	-10.7	-0.35601	0.511454	-3.8	1.58	0.7055
RE-CE-27C	Barreiro HTi	14.8	74.3	24	498	0.512070	0.000006	0.1204	0.707729	0.000006	766	-11.1	-0.38794	0.511465	-3.6	1.52	0.7062
RE-CE-13B	Barreiro HTi	10.3	48.6	15	573	0.512040	0.000009	0.1288	0.706054	0.000009	766	-11.7	-0.34542	0.511394	-5.0	1.70	0.7052
RE-CE-19	Barreiro HTi	8.5	39.7	3	657	0.512091	0.000005	0.1291	0.705865	0.000006	766	-10.7	-0.34367	0.511443	-4.1	1.62	0.7057
MI-BE-87B	Andrelândia	8.2	48.6	57	711	0.511970	0.000006	0.1204	0.707192	0.000008	766	-13.0	-0.38794	0.511365	-3.7	1.41	0.7047
MI-BR-39	Andrelândia	3.0	9.6	7	146	0.512692	0.000007	0.1870	0.715332	0.000037	766	1.1	-0.04929	0.511753	2.0	1.69	0.7138
MI-III-18	Juiz de Fora WPB	10.0	48.4	9	639	0.512059	0.000008	0.1245	0.707242	0.000006	766	-11.3	-0.36717	0.511433	-4.2	1.60	0.7068
PA-BE-137A	Juiz de Fora IAT	8.0	38.8	72	464	0.511425	0.000009	0.1254	0.715975	0.000002	2400	-23.7	-0.36247	0.509441	-1.7	2.58	0.7004
MI-BR-19C	Juiz de Fora IAT	6.1	26.5	12	250	0.511734	0.000005	0.1386	0.717248	0.000008	2400	-17.6	-0.29543	0.509542	0.3	2.43	0.7124
MI-VIII-15	Juiz de Fora IAT	4.2	17.2	2	35	0.512047	0.000008	0.1496	0.712324	0.000009	2400	-11.5	-0.23962	0.509681	3.0	2.16	0.7066

Rb*-Values from geochemical data

Three mafic enclaves with geochemical signatures of convergent tectonic settings (IAT/BAB or CAB), found in the Juiz de Fora Complex, yielded T_{DM} ages between 2.58 Ga and 2.16 Ga, with ε_t between +3.0 and -1.7. These samples display initial $^{87}Sr/^{86}Sr$ ratios between 0.7004 and 0.7124. These results reflect an older convergent juvenile accretion history of the Juiz de Fora complex, as previously reported by Heilbron *et al.* (2010) and Degler *et al.* (2018).

DISCUSSION

Two tectonic settings in the studied area indicated by metabasic rocks

The data presented above, summarized in Table 5, suggest late Tonian (ca. 766 Ma) extensional intraplate magmatism both in the cover and in the basement of the distal segment of the São Francisco paleocontinent passive margin (Andrelândia Group).

The development of the Andrelândia basin in the proximal zone started in the Mesoproterozoic to Neoproterozoic transition, as indicated by the youngest detrital zircons of ca. 0.9 Ma (Valeriano *et al.* 2004, Belém *et al.* 2011) and T_{DM} of interlayered metabasic rocks of ca. 1.0 Ga (Heilbron *et al.* 1989, Frugis & Campos Neto 2018). The new data presented here indicate that the evolution of the distal passive margin lasted at least until late Tonian times.

This late Tonian within-plate magmatism displays within plate basalts (WPB) signatures, with both high-TiO_2 and low-TiO_2 groups, with a few samples showing relatively primitive MORB-like signatures. Mafic magmatic rocks intrude both basement rock associations (Juiz de Fora Complex), as well the cover of distal Andrelândia passive margin (Figs. 12 and 13).

A few samples detected only in the Juiz de Fora Complex display convergent tectonic signatures (IAT to CAB) and older

Table 5. Summary of the new data obtained for mafic rocks of the Barreiro Suite and mafic enclaves of Andrelândia Group and Juiz de Fora Complex.

Mafic groups		U-Pb age (Ga)	$T_{DM(Nd)}$ (Ga)	εNd_t	$^{87}Sr/^{86}Sr(i)$	εHf_t and $T_{DM(Hf)}$
High TiO_2 Barreiro Suite and few mafic enclaves	Intraplate		1.80 to 1.50	-8 to -3	0.7017 to 0.7092	
Low TiO_2 Barreiro suite and enclaves of Juiz de Fora Complex and Andrelândia Group	Intraplate	0.77	1.80 to 1.50	-8 to -3	0.7017 to 0.7092	1.75 to 0.96 Ga, +5.61 to +0.24
Most primitive sample of the Barreiro Suite (RE-BR-28)	Intraplate		0.97	+4	0.7036	
Low TiO_2 enclaves of the Andrelândia group and Juiz de Fora Complex	Morb		1.80 to 1.50	-8 to -3	0.7017 to 0.7092	
Low TiO_2 enclaves of Juiz de For a complex	IATand CAB	2.2 to 2.07	2.58 to 2.16	+3 to -1.7	0.7004 to 0.7124	

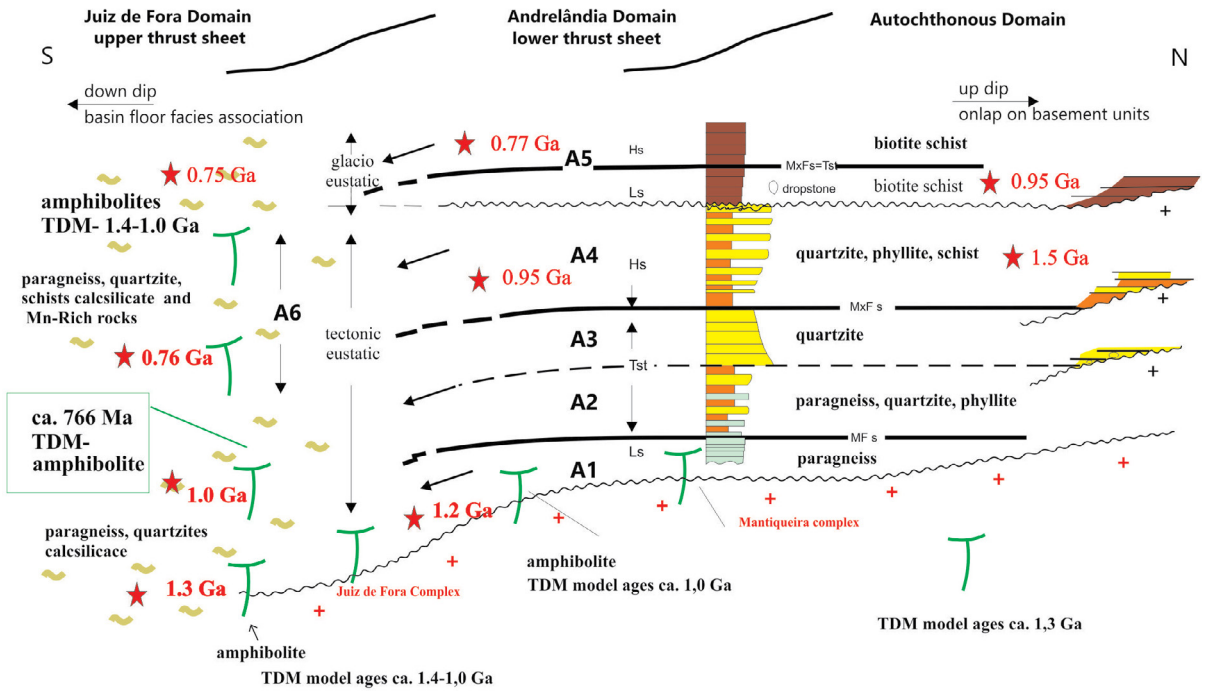

Figure 12. Composite stratigraphic chart for the Andrelândia basin, including proximal (autochthonous and Andrelândia domains) and distal (Andrelândia and Juiz de Fora domains), modified from Ribeiro *et al.* (2013) and Heilbron *et al.* (2017a). Amphibolite data are from this work, Frugis & Campos Neto (2018) and Heilbron *et al.* (1989). Younger detrital zircon was compiled from Valladares *et al.* (2004, 2008), Ribeiro *et al.* (2013), Degler *et al.* (2017), Frugis & Campos Neto (2018).

T_{DM} model ages, indicating that they probably belong to the Paleoproterozoic history of the basement.

Both associations show evidence of Neoproterozoic Brasiliano overprinting, with high deformation textures and granulite facies metamorphism between ca. 619 (this work) and 565 Ma (Duarte 2003, Heilbron & Machado 2003, Bento dos Santos *et al.* 2007, Degler *et al.* 2017).

Correlation with previous data reported for the Andrelândia basin

Previous works have reported combined geochemical and geochronological data for the metabasic rocks interlayered with the metasedimentary rocks of the Andrelândia Basin. In the most proximal region, between Madre de Deus de Minas and Andrelândia towns, southern Minas Gerais State, Gonçalves & Figueiredo (1992) and Paciullo *et al.* (2000) obtained very similar results, with low- and high-TiO_2 amphibolites, pointing to intraplate to MORB-like signatures, suggestive of syn-sedimentary magmatism. These authors suggested that the magmatism evolved in time from high-TiO_2 intraplate rocks in the lower units to MORB signatures in the upper units of the basin. Marins (2000) also reported the same geochemical groups for the amphibolites interlayered within the distal portion of the Andrelândia basin (Raposos Group). The comparison between all the available geochemical data is presented in Figure 13 and provides additional evidence of a major episode of intraplate to E-MORB tholeiitic magmatism between 0.9 Ga and 0.77 Ga associated with the development of the southeastern and eastern São Francisco paleocontinent passive margin.

Tectonic implications for the Neoproterozoic passive margin evolution within the Araçuaí-Ribeira orogenic system

The geochronology data presented herein provide constraints to the timing of evolution of the distal segment of the Andrelândia basin (Raposos Group) from ca. 1.0 Ga to ca. 766 Ma (Fig. 12). This age interval agrees well with the evolution of the Macaúbas Group, located to the north, in the Araçuaí Belt. Other reported coeval intraplate magmatic episodes are the Pedro Lessa suite, the Northern Espinhaço mafic dykes and the Salto da Divisa A-type granites, with ages of 910 to 850 Ma, as well as correlative bimodal volcanic rocks and A-type granites in Africa with ages of 930 to 910 Ma (Pedrosa-Soares & Alkmim 2011, Pedrosa-Soares *et al.* 2000, 2016).

Published ages between ca. 735 Ma and 675 Ma, from the Southern Bahia Alkaline Province, and from the La Louila felsic volcanism in southwest Gabon (≤ 713 Ma) constrain the timing of deposition of the top units of the Macaúbas Group and African correlatives (Pedrosa-Soares & Alkmim 2011). This data indicates that the extensional history of the São Francisco eastern passive margin could have lasted until Cryogenian times, coeval with the development of outboard magmatic arcs eastern wards (Heilbron *et al.* 2008, 2017a).

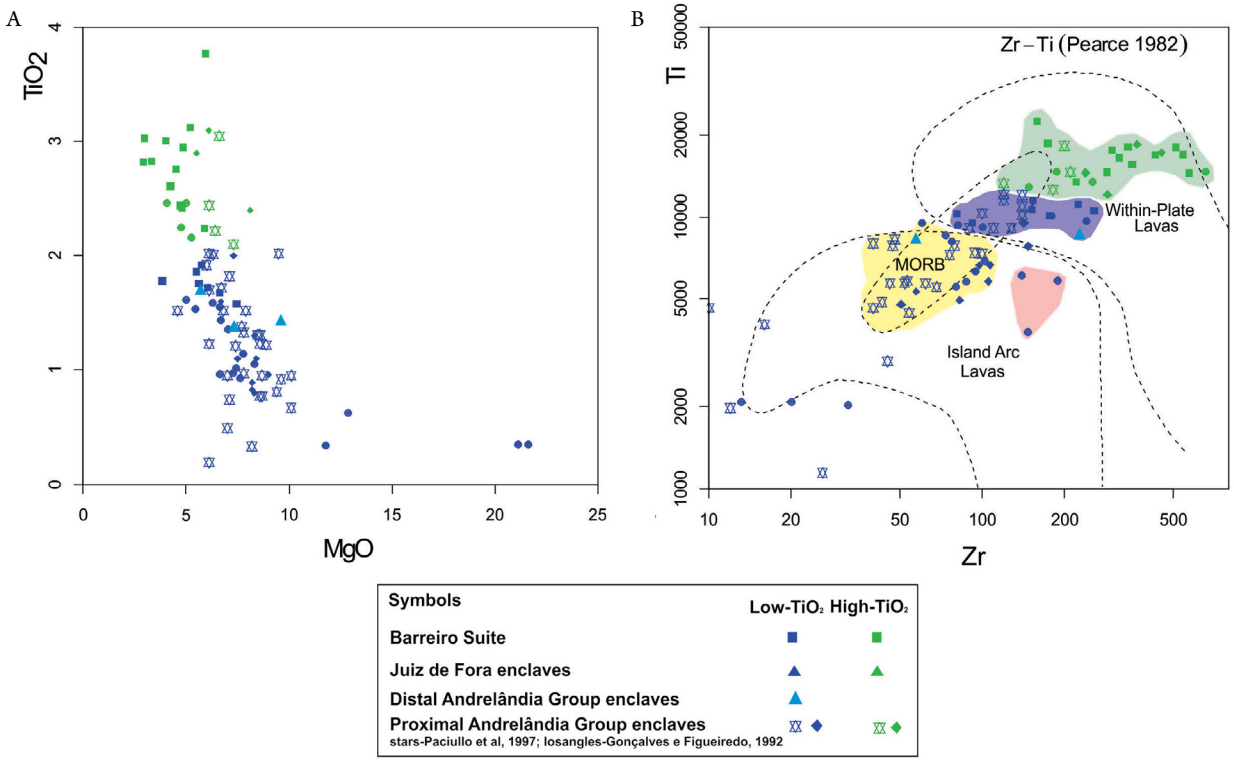

Figure 13. A comparison of new data and previously published data for mafic rocks in the region of the Andrelândia deformed basin units. Proximal data are compiled from Paciullo (1997) and Gonçalves and Figueiredo (1992), compared with our data for the distal part of the basin (Barreiro Suite) and the mafic enclaves of both the Andrelândia Group and the Juiz de Fora Complex. (A) TiO_2 × MgO diagram showing that both proximal and distal samples could be subdivided into the same groups, and (B) plot in the Zi-Ti tectonic diagram of Pearce (1982), with green, blue, yellow and pink fields to show respectively, the intraplate High- and Low-TiO_2 groups, MORB-like samples and a few older mafic enclaves of the Juiz de Fora Complex with arc-related signatures.

CONCLUSIONS

The combination of the data presented herein with previously reported studies for the metabasic rocks of the Ribeira Belts reveals that at least three different episodes of mafic magmatism can be detected in the distal part of the Andrelândia basin and associated basement complexes. The two older episodes are represented by dismembered metabasic rocks found within the orthogranulites of the basement Juiz de Fora Complex and related to the Rhyacian arc (ca. 2.2 to 2.1 Ga) and to Statherian (ca. 1.7 Ga) intraplate magmatism. The youngest episode occurs as dismembered metabasic bodies that intruded both the cover and the basement association, with a late Tonian age of ca. 766 Ma, and clearly displays intraplate signatures associated with the evolution of the distal passive margin (Fig. 13).

An important implication of the characterization of this Late Tonian to Early Cryogenian intraplate metabasic rocks is that they must have shed detrital zircons that have been found sparsely in previous studies on the distal segments of the Andrelândia basin. We suggest that the existence of detrital zircons originated from intraplate magmatic events should be considered in future provenance studies of metasedimentary units of Neoproterozoic succession around the São Francisco craton, rather than necessarily originating from approaching magmatic arcs, as they have been commonly interpreted.

ACKNOWLEDGEMENTS

The authors are grateful to CPRM-PRONAGEO, CNPq and FAPERJ for research funding, and to the technicians of the laboratories from Brasília (UnB-Brazil), LAGIR (UERJ-Brazil) and Notre Dame (USA) universities. Monica Heilbron and Marcela Lobato were granted respectively Senior Visiting Professor and Sandwich PhD CAPES scholarships. Claudio Valeriano acknowledges a scholarship from CNPq (Estágio Senior no Exterior). We also would like to thank the generous revisions of Brendan Murphy, Robert Pankhurst and a third anonymous reviewer, which helped to improve an earlier version of the manuscript.

ARTICLE INFORMATION

Manuscript ID: 20180129. Received on: 11/20/2018. Approved on: 02/19/2019.

M. H. wrote the manuscript, managed the corrections, made the final format of figures and maps, organized and integrated all data, collected samples and did the fieldwork. C. O. contributed to write the manuscript, obtained and discussed the geochemical data, including figures and tables. M. L. discussed the data, ran the U-Pb and Lu-Hf data, made figures and respective tables. I. D. contributed to write the manuscript, helped to process and discussed U-Pb and Lu-Hf. C. V. contributed to write and revise the manuscript, obtained and discussed Sm-Nd data, including tables and figures. E. D. obtained and helped to process and discuss the U-Pb data. A. S. obtained and helped to process and discuss the Hf data. H. B. contributed to field work, maps and geochemical approach, including final version of the figures of geochemistry. F. C. contributed to field work, maps and geochemical approach collected and processed samples and geochronology approach. E. S. contributed to field work and made the geology maps and structural geology approach.

Competing interests: The authors declare no competing interests.

REFERENCES

Alkmim F.F, Kuchenbecker M., Reis H.L.S., Pedrosa-Soares A.C. 2017. The Araçuaí belt. *In*: Heilbron M., Cordani U.G., Alkmim F.F. (eds). São Francisco Craton, Eastern Brazil Tectonic Genealogy of a Miniature Continent. 1 ed. Springer, v. 1, 251-276.

Almeida F.F.M. de, Hasui Y., Brito Neves B.B., Fuck R.A. 1981. Brazilian structural provinces: an introduction. *Earth-Science Reviews*, **17**(1-2):1-29. https://doi.org/10.1016/0012-8252(81)90003-9

Andersen T., Andersson U.B., Graham S., Åberg G., Simonsen S.L. 2009. Granitic magmatism by melting of juvenile continental crust: new constraints on the source of Paleoproterozoic granitoids in Fennoscandia from Hf isotopes in zircon. *Journal of the Geological Society*, **166**(2):233-247. http://dx.doi.org/10.1144/0016-76492007-166

Belém J., Pedrosa-Soares A.C., Noce C.M., Silva L.C., Armstrong R., Fleck A., Gradim C.T., Queiroga G.N. 2011. Bacia precursora versus bacias orogênicas: exemplos do Grupo Andrelândia com base em datações U-Pb (LA-ICP-MS) em zircão e análises litoquímicas. *Geonomos*, **19**(2):224-243. https://doi.org/10.18285/geonomos.v19i2.55

Bento dos Santos T., Munhá J., Tassinari C., Fonseca P., Dias Neto C. 2007. Thermochronological evidence for long-term elevated geothermal gradients in Ribeira Belt, SE Brazil. *Geochimica et Cosmochimica Acta*, **71**(15 Suppl. 1):A79.

Bouvier A., Vervoort J.D., Patchett P.J. 2008. The Lu–Hf and Sm–Nd isotopic composition of CHUR: Constraints from unequilibrated chondrites and implications for the bulk composition of terrestrial planets. *Earth and Planetary Science Letters*, **273**(1-2):48-57. https://doi.org/10.1016/j.epsl.2008.06.010

Boynton WV. 1984. Geochemistry of Rare Earth Elements: Meteorite Studies. *In*: Henderson P. (eds). *Rare Earth Element Geochemistry*. Elsevier, New York, p. 63-114.

Bühn B., Pimentel M.M., Matteini M., Dantas E. 2009. High spatial resolution analysis of Pb and U isotopes for geochronology by laser ablation multicollector inductively coupled plasma mass spectrometry inductively coupled plasma mass spectrometry (LA-MC-ICPMS). *Anais da Academia Brasileira de Ciências*, **81**(1):99-114. http://dx.doi.org/10.1590/S0001-37652009000100011

Campos Neto M.C. 2000. Orogenic systems from Southwestern Gondwana, an approach to Brasiliano-Pan African cycle and orogenic collage in southeastern Brazil. *In*: Cordani U.G., Milani E.J., Thomaz Filho A., Campos D.A. (eds.), *Tectonic Evolution of South America*. Rio de Janeiro, SBG.

Campos Neto M.C., Basei M.A.S., Janasi V.A., Moraes R. 2011. Orogen migration and tectonic setting of the Andrelândia Nappe system: an Ediacaran western Gondwana collage, south of São Francisco Craton. *Journal of South American Earth Sciences*. **32**(4):393-406.

Campos Neto M.C., Basei M.A.S., Vlach S.R.F., Caby R., Szabo G.A.J., Vasconcelos P. 2004. Migração de orógenos e superposição de orogêneses: Um esboço da colagem brasiliana no sul do Cráton do São Francisco, SE-Brasil. *Boletim do Instituto de Geociências/USP*, **4**:13–40.

Coelho M.B., Trouw R.A.J., Ganade de Araújo C.E., Vinagre R., Mendes J.C., Sato K. 2017. Constraining timing and P-T conditions of continental collision and late overprinting in the Southern Brasília Orogen (SE-Brazil): U-Pb zircon ages and geothermobarometry of the Andrelândia Nappe System. *Precambrian Research*, **292**:194-215. https://doi.org/10.1016/j.precamres.2017.02.001

Cox K.G. 1989. The role of mantle plumes in the development of continental drainage patterns. *Nature*, **342**:873-877. http://dx.doi.org/10.1038/342873a0

De la Roche H., Leterrier J., Grand Claude P., Marchal M. 1980. A classification of volcanic and plutonic rocks using R1--R2 diagrams and major element analyses - its relationships with current nomenclature. *Chemical Geology.,* **29**:183-210.

De Paolo D.J. 1981. A neodymium and strontium isotopic study of the Mesozoic calc-alkaline granitic batholiths of the Sierra Nevada and Peninsular Ranges, California. *Journal of Geophysical Research*, **86**(B11):10470-10488. https://doi.org/10.1029/JB086iB11p10470

Degler R., Pedrosa-Soares A.C., Dussin I., Queiroga G., Schulz B. 2017. Contrasting provenance and timing of metamorphism from paragneisses of the Araçuaí-Ribeira orogenic system, Brazil: Hints for Western Gondwana assembly. *Gondwana Research*, **57**:30-50. http://dx.doi.org/10.1016/j.gr.2017.07.004

Degler R., Pedrosa-Soares A.C., Novo T., Tedeschi M., Silva L.C., Dussin I., Lana C. 2018. Rhyacian-Orosirian isotopic records from the basement of theAraçuaí-Ribeira orogenic system (SE Brazil): Links in the Congo-São Francisco paleocontinent. *Precambrian Research*, **317**:179-195. http://dx.doi.org/10.1016/j.precamres.2018.08.018

Duarte B., Heilbron M., Nogueira J.R., Tupinambá M., Eirado L.G., Valladares C., Almeida J.C.H., Guia C. 2003. Geologia das Folhas Juiz de Fora e Chiador. *In*: Pedrosa-Soares A.C., Noce C.M., Trouw R., Heilbron M. (coords.). *Projeto Sul de Minas*. Belo Horizonte, COMIG/SEME, v. 1. p. 153-258.

Frugis G. & Campos Neto M. 2018. Eastern Paranapanema and Southern São Francisco orogenic margins: Records of enduring Neoproterozoic oceanic convergence and collision in the Southern Brasília Orogen. *Precambrian Research*, **308**:35-57.

Gonçalves M.L. & Figueiredo M.C.H. 1992. Geoquímica dos Anfibolitos de Santana do Garambéu (MG): Implicações Tectônicas sobre a Evolução do Grupo Andrelândia. *Geochimica Brasiliensis*, **6**(2):127-140.

Griffin W.L., Pearson N.J., Belousova E., Jackson S.E., van Achterbergh E., O'Reilly S.Y., Shee S.R. 2000. The Hf isotope composition of cratonic mantle: LAM-MC- ICPMS analysis of zircon megacrysts in kimberlites. *Geochimica et Cosmochimica Acta*, **64**(1):133-147.https://doi.org/10.1016/S0016-7037(99)00343-9

Heilbron H., Cordani U., Alkmim F., Reis H. 2017a. Tectonic Genealogy of a Miniature Continent. *In*: Heilbron M., Cordani U.G., Alkmim F.F. (eds.), *São Francisco Craton, Eastern Brazil*. Regional Geology Reviews. Berlin, Springer.

Heilbron M., Duarte B.P., Nogueira J.R. 1998. The Juiz de Fora complex of the Central Ribeira belt, SE Brazil: a segment of Paleoproterozoic granulitic crust thrust during the Pan-African Orogen. *Gondwana Research*, **1**(3):373-381. http://dx.doi.org/10.1016/S1342-937X(05)70853-4

Heilbron M., Duarte B.P., Valeriano C., Simonetti A., Machado N., Nogueira J. 2010. Evolution of reworked Paleoproterozoic basement rocks within the Ribeira belt (Neoproterozoic), SE-Brazil, based on U Pb geochronology: Implications for paleogeography reconstructions of the São Francisco-Congo paleocontinent. *Precambrian Research*, **178**(1):136-148. http://dx.doi.org/10.1016/j.precamres.2010.02.002

Heilbron M., Gonçalves M.L., Teixeira W., Trouw R.A.J., Padilha A., Kawashita K. 1989. Geocronologia da área entre Lavras, São João del Rei, Lima Duarte e Caxambu. *Anais da Academia Brasileira de Ciências*, **61**(2):177-199.

Heilbron M. & Machado N. 2003. Timing of terrane accretion in the Neoproterozoic-Eopaleozoic Ribeira belt (se Brazil). *Precambrian Research*, **125**(1-2):87-112.

Heilbron M., Pedrosa-Soares A.C., Campos Neto M., Silva L.C., Trouw R.A.J., Janasi V.C. 2004. A Província Mantiqueira. *In*: Mantesso-Neto V., Bartorelli A., Carneiro C.D.R., Brito Neves B.B. (eds.), *O Desvendar de um Continente:* A Moderna Geologia da América do Sul e o Legado da Obra de Fernando Flávio Marques de Almeida. São Paulo, Beca, p. 203-204.

Heilbron M., Ribeiro A., Valeriano C.M., Paciullo F., Almeida J.C.H., Trouw R., Tupinambá M., Silva L.G.E. 2017a. The Ribeira belt. *In*: Heilbron M., Cordani U.G., Alkmim F. (eds.), *São Francisco Craton, Eastern Brazil Tectonic Genealogy of a Miniature Continent*. Berlin, Springer, v. 1, p. 277-304.

Heilbron M., Tupinambá M., Almeida J.C.H., Valeriano C., Gontijo A., Silva T.M., Menezes P.T.L., Mane M., Palermo N., Pereira R.M. 2012. Introdução. *In*: Heilbron M. (eds.), *Geologia e recursos minerais da folha Santo Antônio de Pádua SF.* 26-X-D-VI, escala 1:100.000. Belo Horizonte, CPRM, v. 1, p. 17-21.

Heilbron M., Valeriano C.M., Almeida J.C.H., Eirado L.G. 2107b. *Geologia e Recursos Minerais do estado do Rio de Janeiro*. 1. ed. Brasília, CPRM, v. 1, 182p.

Heilbron M., Valeriano C.M., Tassinari C.C.G., Almeida J., Tupinambá M., Siga O., Trouw R. 2008. Correlation of Neoproterozoic terranes between the Ribeira Belt, SE Brazil and its African counterpart: comparative tectonic evolution and open questions. *Geological Society Special Publications*, **294**:211-237. https://doi.org/10.1144/SP294.12

International Union of Pure and Applied Chemistry. 1998. Commission on Atomic Weights and Isotopic Abundances. Isotopic Compositions of the Elements 1997. *Pure and Applied Chemistry*, **70**(1):217-235.

Irvine T.N. & Baragar W.R.A. 1971. A guide to the chemical classification of the common volcanic rocks. *Canadian Journal of Earth Sciences*, **8**(5):523-548. https://doi.org/10.1139/e71-055

Janoušek V., Farrow C.M., Erban V. 2006. Interpretation of whole-rock geochemical data in igneous geochemistry: introducing Geochemical Data Toolkit (GCDkit). *Journal of Petrology*, **47**(6):1255-1259. https://doi.org/10.1093/petrology/egl013

Le Bas M.J., Le Maitre R.W., Streckeisen A., Zanettin B. 1986. A chemical classification of volcanic rocks based on the total alkali–silica diagram. *Journal of Petrology*, **27**(3):745-750. http://dx.doi.org/10.1093/petrology/27.3.745

Le Maitre R.W., Bateman P., Dudek A., Keller J., Lameyre J., LeBas M.J., Sabine P.A., Schmid R., Sorensen H., Streckeisen A., Wooley A.R., Zanettin B. 1989. *A classification of igneous rocks and glossary of terms*. Oxford, Blackwell.

Ludwig K.R. 2003. Isoplot 3.00, A Geochronological Toolkit for Excel: *Berkeley Geochronology Center Special Publication* No. 4.

Machado N., Valladares C., Heilbron M., Valeriano C. 1996. U/Pb Geochronology Of Central Ribeira Belt: Implications For The Evolution Of Brasiliano Orogeny. *Precambrian Research*, **79**(3):347-361.

Marins G. 2000. *Petrologia dos Anfibolitos do Domínio Juiz de Fora e da Klippe Paraíba do Sul, no Setor Central da Faixa Ribeira*. MS Dissertation, Programa em Análise de Bacias e Faixas Móveis, Universidade do Estado do Rio de Janeiro, Rio de Janeiro.

Meschede M. 1986. A method of discriminating between different types of mid-ocean ridge basalts and continental tholeiites with the Nb-Zr-Y diagram. *Chemical Geology*, **56**:207-218.

Noce C.M., Pedrosa-Soares A.C., Silva L.C., Armstrong R., Piuzana D. 2007. Evolution of polycyclic basement complexes in the Araçuaí orogen, based on U–Pb SHRIMP data: Implication of Brazil-Africa links in Paleoproterozoic time. *Precambrian Research*, **159**:60-78.

Noce C.M., Romano A.W., Pinheiro C.M., Mol V.S., Pedrosa-Soares A.C. 2003. Geologia das Folhas Ubá e Muriaé. *In*: Pedrosa-Soares A.C. Noce CM, Trouw R, Heilbron M.. (eds.), *Geologia e Recursos Minerais do Sudeste Mineiro*. Belo Horizonte, COMIG, p. 623-659.

Paciullo F.V.P. 1997. A Sequência Deposicional Andrelândia. Doctoral Thesis, Instituto de Geociências, Universidade Federal do Rio de Janeiro, Rio de Janeiro.

Paciullo F.V.P., Ribeiro A., Andreis R.R., Trouw R.A.J. 2000. The Andrelândia Basin, a Neoproterozoicintra-plate continental margin,southern Brasília Belt. *Revista Brasileira de Geociências*, **30**(1):200-202.

Pearce J.A. 1982. Trace element characteristics of lavas from destructive plate boundaries. *In*: Thorpe R.S. (ed.), *Andesites:* orogenie andesites and related rocks. Chichester, Wiley, p. 525-548.

Pearce J.A. 1983. The role of sub-continental lithosphere in magma genesis at destructive plate margins. *In*: Hawkesworth C.J. & Norry M.J. (eds.), *Continental basalts and mantle xenoliths*. Nantwich: Shiva, p. 230-249.

Pearce J.A. 1987. An expert system for the tectonic characterization of ancient volcanic rocks. *Journal of Volcanology and Geothermal Research*, **32**(1-3):51-65. https://doi.org/10.1016/0377-0273(87)90036-9

Pearce J.A. & Cann J.R. 1973. Tectonic setting of basic volcanic rocks determined using trace element analysis. *Earth and Planetary Science Letters*, **19**(2):290-300. http://dx.doi.org/10.1016/0012-821X(73)90129-5

Pearce T.H., Gorman B.E., Birkett T.C. 1975. The TiO2-K2O-P2O5 diagram: a method of discriminating between oceanic and non-oceanic basalts. *Earth and Planetary Science Letters*, **24**(3):419-426. https://doi.org/10.1016/0012-821X(75)90149-1

Pedrosa-Soares A.C. & Alkmim F.F. 2011. How many rifting events preceded the development of the Araçuaí-West Congo orogen? *Geonomos*, **19**(2). https://doi.org/10.18285/geonomos.v19i2.56

Pedrosa-Soares A.C., Alkmim F.F., Tack L., Noce C.M., Babinski M., Silva L.C., Martins-Neto M. 2008. Similarities and differences between the Brazilian and African counterparts of the Neoproterozoic Araçuaí–West Congo Orogen. *In*: Pankhurst J.R., Trouw R.A.J., Brito Neves B.B., De Wit M.J. (eds.).*West Gondwana: Pre-Cenozoic Correlations across the South Atlantic Region*. Geological Society, London, Special Publications, 294, p. 153-172.

Pedrosa-Soares A.C., Dussin I., Nseka P., Baudet D., Fernandez-Alonso M., Tack L. 2016. Tonian rifting events on the Congo-São Francisco paleocontinent: New evidence from U-Pb and Lu-Hf data from the Shinkakasa plutonic complex (Boma region, West Congo Belt, Democratic Republic of Congo). *In*: International Geologica Belgica Meeting. Mons, 5., Belgium. *Abstract Book…*, p. 44.

Pedrosa-Soares A.C., Vidal P., Leonardos O.H., Brito-Neves B.B. 1998. Neoprotero-zoic oceanic remnants in eastern Brazil: further evidence and refutation of an exclusively ensialic evolution for the Araçuaí–West Congo orogen. *Geology*, **26**(6):519-522. https://doi.org/10.1130/0091-7613(1998)026%3C0519:NORIEB%3E2.3.CO;2

Pedrosa-Soares A.C., Wiedemann-Leonardos C.M. 2000. Evolution of the Araçuaí Belt and its connection to the Ribeira Belt, Eastern Brazil. *In*: Cordani U., Milani E., Thomaz-Filho A., Campos D.A. (eds.), *Tectonic Evolution of South America*. São Paulo, Sociedade Brasileira de Geologia, p. 265-285.

Ribeiro A., Teixeira W., Dussin I.A., Ávila C.A., Nascimento D. 2013. U-Pb LA-ICP-MS detrital zircon ages of the São João del Rei and Carandaí basins: New evidence of intermittent Proterozoic rifting in the São Francisco paleocontinent. *Gondwana Research*, **24**(2):713-726. http://dx.doi.org/10.1016/j.gr.2012.12.016

Ribeiro A., Trouw R.A.J, Andreis R.R., Paciullo F.V.P., Valença J.G. 1995. Evolução das bacias proterozóicas e o termo-tectonismo brasiliano na margem sul do cráton do São Francisco. *Revista Brasileira de Geociências*, **25**:235-248.

Rollinson H. 1993. *Using geochemical data:* evaluation, presentation, interpretation. United Kingdom, Pearson Education Limited, Longman Group.

Rubatto D. 2017. Zircon: The Metamorphic Mineral. *In*: Kohn M.J., Engi M., Lanari P. (eds.), Petrochronology. *Reviews in Mineralogy and Geochemistry*, **83**:261-289.

Saccani E. 2015. A new method of discriminating different types of post-Archean ophiolitic basalts and their tectonic significance using Th-Nb and Ce-Dy-Yb systematics. *Geoscience Frontiers*, **6**(4):481-501. https://doi.org/10.1016/j.gsf.2014.03.006

Shervais J.V. 1982. Ti-V plots and the petrogenesis of modern and ophiolitic lavas. *Earth and Planetary Science Letters*, **59**:101–118.

Silva L.C., Armstrong R., Noce C.M., Carneiro M., Pimentel M., Pedrosa-Soares A.C., Leite C., Vieira V.S., Silva M., Paes V., Cardoso-Filho J. 2002. Reavaliação da evolução geológica em terrenos pré-cambrianos brasileiros com base em novos dados U-Pb SHRIMP; parte II: Orógeno Araçuaí, Cinturão Móvel Mineiro e Cráton São Francisco Meridional. *Revista Brasileira de Geociências*, **32**(4):513-528.

Simonetti A., Neal C.R. 2010. In-situ chemical, U–Pb dating, and Hf isotope investigation of megacrystic zircons, Malaita (Solomon Islands): Evidence for multi-stage alkaline magmatic activity beneath the Ontong Java Plateau. *Earth and Planetary Science Letters*, **295**:251-261. http://dx.doi.org/10.1016/j.epsl.2010.04.004

Söderlund U., Patchett J.P., Vervoort J.D., Isachsen C.E. 2004. The 176Lu decay constantdetermined by Lu–Hf and U–Pb isotope systematics of Precambrian mafic intrusions. *Earth and Planetary Science Letters*, **219**(3-4):311-324. https://doi.org/10.1016/S0012-821X(04)00012-3

Stacey J.S. & Kramers J.D. 1975. Approximation of terrestrial lead isotope evolution by a two-stage model. *Earth Planet Science Letters,* **26**:207-221.

Sun S. & McDonough W.F. 1989. Chemical and isotopic systematics of oceanic basalts: implications for mantle composition and processes. *In*: Saunders A.D., Norry M.J. (eds.), *Magmatism in the Ocean Basins*. London, Geological Society, p. 313-345.

Tanaka T., Togashi S., Kamioka H., Amakawa H., Kagami H., Hamamoto T.,Yuhara M., Orihashi Y., Yoneda S., Shimizu H., Kunimaru T., Takahashi K., Yanagi T., Nakano T., Fujimaki H., Shinjo R., Asahara Y., Tanimizu M., Dragusanu C. 2000. JNdi-1: a neodymium isotopic reference in consistency with Lajolla neodymium. *Chemical Geology*, **168**:279-281. http://dx.doi.org/10.1016/S0009-2541(00)00198-4

Tedeschi M., Pedrosa-Soares A.C., Dussin I., Lanarid P., Novo T., Pinheiro M.A., Lana C., Peters D. 2018. Protracted zircon geochronological record of UHT garnet-free granulites in the Southern Brasília orogen (SE Brazil): Petrochronological constraints on magmatism and metamorphism. *Precambrian Research*, **316**:101-126. http://dx.doi.org/10.1016/j.precamres.2018.07.023

Trouw R.A.J., Heilbron M., Ribeiro A., Valeriano C., Paciullo F., Almeida J.C.H., Tupinambá M. 2000. The Central Segment of the Ribeira belt. *In*: Cordani U., Milani E., Thomaz-Filho A., Campos D. (eds.). *Geotectonics of South America*. Rio de Janeiro, CPRM, v. 1, p. 287-310.

Trouw R.A.J., Peternel R., Ribeiro A., Heilbron M., Vinagre R., Duffles P., Trouw C.C., Fontainha M., Kussama H.H. 2013. A new interpretation for the interference zone between the southern Brasília belt and the central Ribeira belt, SE Brazil. *Journal of South American Earth Sciences*, **48**:43-57.

Valeriano C.M., Machado N., Simonetti A., Valladares C.S., Seer H.J., Simões L.S.A. 2004. U Pb geochronology of the southern Brasília belt (SE-Brazil): sedimentary provenance, Neoproterozoic orogeny and assembly of West Gondwana. *Precambrian Research*, **130**(1/4):27-55.

Valeriano C.M., Vaz G.S., Medeiros S.R., Neto C.C.A., Ragatky C.D. 2008. The Neodymium isotope composition of the JNdi-1 oxide reference material: results from the LAGIR Laboratory, Rio de Janeiro. *In*: South American Symposium on Isotope Geology, 6., San Carlos de Bariloche, Argentina. *Proceedings…* p. 1-2. 1 CD-ROM.

Valladares C.S., Machado N., Heilbron M., Duarte B.P., Gauthier G. 2008. Sedimentary provenance in the central Ribeira belt based on laser-ablation ICPMS $^{207}Pb/^{206}Pb$ zircon ages. *Gondwana Research*, **13**:516-526. http://dx.doi.org/10.1016/j.gr.2007.05.013

Valladares C.S., Machado N., Heilbron M., Gauthier G. 2004. Ages of detrital zircon from siliciclastic successions south of the São Francisco Craton, Brazil: implications for the evolution of Proterozoic basin. *Gondwana Research*, **7**(4):913-921. https://doi.org/10.1016/S1342-937X(05)71074-1

Xia L. & Li X. 2019. Basalt geochemistry as a diagnostic indicator of tectonic setting. *Gondwana Research*, **65**:43-67. http://dx.doi.org/10.1016/j.gr.2018.08.006

Westin A. & Campos Neto M.C. 2013. Provenance and tectonic setting of the external nappe of the Southern Brasília Orogen. *Journal of South American Earth Sciences*, **48**:220-239. http://dx.doi.org/10.1016/j.jsames.2013.08.006

Wilson M. 1989. *Igneous petrogenesis:* a global tectonic approach. London, Unwin Hyman, 466 p.

Wise S.A. & Waters R.L. 2007. Certificate of analysis standard reference material® 987 Strontium Carbonate (Isotopic Standard). NIST National Institute of Standards & Technology, 2 p. Available at: <https://www.nist.gov>.

Zeh A., Gerdes A., Will T.M., Frimmel H.E. 2010. Hafnium isotope homogenization during metamorphic zircon growth in amphibolite-facies rocks: examples from the Shackleton Range (Antarctica). *Geochimica et Cosmochimica Acta*, **74**(16):4740-4758. http://dx.doi.org/10.1016/j.gca.2010.05.016